NASA Technical Memorandum 81558

NASA-TM-81558 19800022893

REVERSE THRUST PERFORMANCE OF THE QCSEE VARIABLE PITCH TURBOFAN ENGINE

N. E. Samanich, D. C. Reemsnyder, and H. E. Bloomer
Lewis Research Center
Cleveland, Ohio

Prepared for the
Aerospace Congress
sponsored by the Society of Automotive Engineers
Los Angeles, California, October 13-16, 1980

NASA

SHORT-HAUL AIRCRAFT HAVE BEEN PROPOSED as one solution to airport congestion a number of years ago. In principle, these aircraft would operate out of numerous existing short runway airfields, and would thereby alleviate the increasing traffic problem at major terminals. In 1974, NASA-Lewis awarded a contract to The General Electric Company to design, fabricate and test two Quiet, Clean, Short-Haul, Experimental Engines (QCSEE). One propulsion system was designed for an Under-the-Wing (UTW) externally blown flap application; the other was configured for Over-the-Wing (OTW) upper-surface blowing. Major objectives of the program were to develop the technology needed to meet the stringent noise, exhaust emissions, performance, weight and transient thrust requirements of future short-haul aircraft. The contractor phase of the program was completed in 1978 and results reported in (1, 2)*. Subsequently NASA-Lewis evaluated complete engine systems with representative powered-lift wing segments (3). Testing included acoustic evaluation of bulk absorber material (4), UTW reverse thrust and forward-to-reverse transient tests. Testing at Lewis was completed in 1979.

Noise requirements for short-haul aircraft and the QCSEE program dictated that a low-pressure ratio, high-bypass ratio fan be used, especially for under-the-wing installation. Studies have indicated that for such installations, engines designed with variable-pitch fans for reverse thrust (5, 6) are superior to those with fixed pitch fans and conventional reversers. The potential advantage of using variable-pitch fans is the elimination of the conventional heavy, high-maintenance, target or cascade thrust-reversal hardware plus the added benefit of improved thrust response time (5, 6). One of the potential problems in operation of variable pitch fans is difficulty in establishing reverse thrust at certain reverse blade angles (7, 8). This problem is aggravated when reversing with forward velocity. However, operational techniques during forward-to-reverse transients, such as blade angle overshoot, have been shown to be effective in reducing the time to establish reverse thrust (7, 8).

During UTW engine steady-state reverse thrust testing at General Electric, turbine temperature limit was reached before the reverse thrust goal of 35% of takeoff thrust was achieved (9, 10). Although removing the aft fan duct acoustic splitter improved the thrust 2%, from 25% to 27% of takeoff thrust, further improvement was desirable. Early model tests (11) indicated that the fan nozzles, if flared to about 30° did provide reasonable pressure recovery when used as inlets. Later testing (12) showed that pressure recovery of these flared inlets could be adversely affected by serrations cut into the leading edge of the inlets. In the reverse position, the QCSEE fan nozzle is flared to about 30°, but sizeable openings exist between the four flaps and between the flaps and main nacelle in the hinge plane.

---

*Numbers in parentheses designate references at end of paper.

In an attempt to evaluate the effect of these openings on reverse performance, a fixed 30° half-angle conical exlet having the same flap length and trailing edge sharpness was fabricated and tested on the QCSEE UTW engine. Steady-state reverse testing reported herein included back-to-back tests with the fixed 30° exlet and the movable flaps (QCSEE). The engine was tested over a range of fan speeds and reverse fan blade angles. Measurements included thrust, fan and core speeds, fan blade angle, and pressure and temperature profiles before and behind the fan rotor and at the compressor face.

The NASA test program culminated with an evaluation of the forward-to-reverse thrust transient characteristics of the QCSEE engine. All transients included an automatic change in the QCSEE four-flap fan nozzle from a forward thrust setting (convergent nozzle) to an open, ~ 30° flare position for reverse. Simultaneously, the fan blades were rotated through "stall" from forward thrust fan blade angles (β_F = +5 to -7°) to reverse thrust blade angles (β_F = -97 to -112°). Transients were initiated from nominal forward idle, approach and takeoff power to various levels of reverse thrust. Other variations included final reverse blade angle, blade angle overshoot and fuel scheduling during the transients. Typical overall sound pressure levels during the transients were also obtained.

This report discusses the results of steady-state reverse tests of two reverse inlet (exlet) configurations and forward-to-reverse transient tests of the QCSEE UTW engine conducted at the Lewis Research Center.

UTW ENGINE CHARACTERISTICS

The UTW engine is an advanced technology, experimental turbofan built around an existing advanced core. The technical advances emphasize such environmental factors as low noise and exhaust emissions. Performance is improved primarily by reducing engine weight to achieve a high engine thrust-weight ratio.

UTW ENGINE DESIGN CHARACTERISTICS - A summary of the QCSEE UTW engine technical goals are presented in Table 1 for a four-engine commercial transport aircraft. Because of the importance of low noise to any future aircraft and particularly short-haul powered-lift aircraft, very stringent goals were established with the takeoff and approach noise level set at 95 EPNdB. The under-the-wing engine installation results in direct impingement of the exhaust jet on the wing flap and the resulting jet/flap interaction noise is a major contributor to the total noise signature. As shown in Fig. 1, a very low fan pressure ratio (jet velocity) was required and was selected to keep this noise source about 3 dB below the total system noise for a balanced acoustic design.

The UTW experimental propulsion system shown in Fig. 2 was designed (13) to provide 81,400 N (18,300 lb) of uninstalled thrust and 77,400 N (17,400 lb) of installed forward thrust at takeoff on a 305.6 K (90°F) day. Reverse thrust goal was set at 35% of forward takeoff thrust.

Specific UTW engine features include: a composite structure high Mach (accelerating) inlet; a gear-driven, variable-pitch fan with composite fan blades; a composite fan frame; an acoustically treated fan duct with an acoustic splitter ring; a variable-geometry fan exhaust nozzle, an advanced (F101) core engine and low pressure turbine; an acoustically treated core exhaust nozzle; top-mounted engine accessories; and a digital electronic control system combined with a hydromechanical fuel control. Critical aerodynamic design parameters are listed in Table 2. The UTW engine has a high bypass ratio of 11.8 and a low fan pressure ratio at takeoff of 1.27.

The UTW engine requires control of four variables; fuel flow, fan blade angle, fan nozzle area and core compressor stator angle. The control system incorporates two basic control components, a modified hydromechanical fuel control and an engine-mounted digital electronic control designed specifically for the QCSEE engines (14). A primary requirement of the control system was the capability of achieving a thrust response of 1.0 sec for approach-to-takeoff thrust and 1.5 sec for approach-to-reverse thrust. During operation, fuel flow controls engine pressure ratio (compressor discharge pressure/inlet total pressure - variables closely related to thrust); fan blade angle controls fan speed, and the fan nozzle area controls inlet Mach number (a key inlet noise parameter). The fan blade variable pitch actuation system was a hydraulically powered ball spline design described in (13).

Acoustic design parameters are listed in Table 3 and acoustic features of the engine are shown in Fig. 3.

UTW ENGINE PERFORMANCE CHARACTERISTICS - A summary of previous GE and NASA test results (1,3) is listed in Table 4. Acoustic tests at NASA (3) of the UTW engine with representative powered-lift wing flap sections indicate peak 152 m (500 ft.) sideline noise of 98.5 and 99.7 EPNdB at approach and takeoff, respectively along with a 2.59 sq km (1.0 sq. mile) 95 EPNdB contour area. Although these values are above the 95 EPNdB and 1.29 sq km (0.5 sq mile) contour area goals, they are substantially lower than any commercial aircraft in service today.

The pollution, forward thrust, specific fuel consumption and thrust-to-weight goals were all met or exceeded. Although the UTW engine failed to meet the 610 m (2000 ft) runway reverse thrust goal of 35% of takeoff thrust, it did produce about 27% reverse thrust, and this might be sufficient to decelerate an aircraft on a 915 m (3000 ft.) runway. The approach-to-takeoff forward thrust transient was not attempted due to fan overspeed indications during lower power transients.

APPARATUS AND PROCEDURE

The UTW variable pitch turbofan engine was tested for reverse performance at a NASA Lewis outdoor engine test stand. Detailed instrumentation, data reduction, and test procedures were incorporated to define steady-state reverse thrust performance and forward-to-reverse thrust transient characteristics.

TEST FACILITY - The engine test stand (Fig. 4 and 5) was designed specifically for test of the QCSEE engines. Specific attention was given to the proximity of the ground plane and stand structure to the inlet and exit planes. These could cause flow turbulence and flow distortion resulting in high blade stress and/or noise generation. Engine centerline was 4.6 m (15 ft) above grade. The stand had separable lower and upper structure. A compact "A" frame upper structure straddled and held the engine (top mounts) and all its accessories. The stand was designed to enable measurement of forward, reverse and side loads. The engine upper stand structure was hung from flexure plates and steady-state thrust was measured by load cells. The outdoor test stand was located at the NASA Lewis Engine Noise Test Facility immediately adjacent to Cleveland Hopkins Airport.

ENGINE TEST CONFIGURATION - A schematic of the reverse thrust configuration along with engine station designations is shown in Fig. 6 and symbols are defined in Appendix A. In the reverse thrust mode, flow enters the engine at the fan nozzle (exlet), passes through the aft fan duct and fan bypass outlet guide vanes and then separates into two streams; one stream passing through the fan rotor and discharging out the engine inlet, and the other stream turning 180° and entering the gooseneck to the core compressor. A photograph of the 6-foot diameter QCSEE fan rotor is shown in Fig. 7. Although the QCSEE design was capable of fan blade pitch change in either direction (Fig. 8), reverse through stall was found to provide improved performance (7) and therefore was used in these tests. In this direction the blades are "opened" about 100° (β_F = -100°) from the forward thrust design blade angle (β_F = 0°).

During reverse operation, the QCSEE fan nozzle is in the flared position (Fig. 9 and 10) and sizeable openings exist between the four flaps and between the flaps and main nacelle in the hinge plane. Edges at the openings are relatively sharp. In an attempt to evaluate the effect of these openings on reverse performance, a fixed 30° half-angle conic exlet having the same flap length and trailing edge sharpness was fabricated and tested. A schematic of the fixed 30° exlet is shown in Fig. 11 and a photograph of it "on test" is shown in Fig. 12. Steady-state reverse testing reported herein included back-to-back tests with the fixed 30° exlet and the movable flaps (QCSEE). All forward-to-reverse transients were made with the movable flaps.

Since noise measurements were not of primary importance in these tests, the acoustic configuration used was the same as that tested immediately preceding this final test series. The acoustic configuration included the accelerating high Mach composite inlet with single-degree-of-freedom (SDOF) wall treatment, treated (bulk absorber) fan duct, and a multi phased stacked SDOF core suppressor. The acoustic fan duct splitter ring was removed. This configuration is described in detail in (4) and was designated as acoustic configuration 3.

INSTRUMENTATION - Because of the unique and rather complex nature of the QCSEE UTW engine, an abnormally large number of steady-state and transient pieces of information were obtained. Details of the instrumentation are presented in (9, 10), and only the pertinent instrumentation is discussed below:

1. Operational Safety Instrumentation - Pressures and/or temperatures in the lubrication and hydraulic system, cooling air supply, oil cooler, fuel system, bearings and seals, reduction gear and in high temperature regions were monitored.

2. Dynamic Instrumentation - Stress and vibration levels were continually monitored on selected fan blades, compressor inlet rakes, the slip ring strut, nozzle flap links, fan frame, fan OGV island, and on various locations on the fan doors. Vibration information was also continually gathered on all critical engine bearings, the accessory gear box, compressor case and the digital control. In an attempt to measure true engine thrust transient response, the two engine thrust links attaching the engine to the facility mounts were removed and replaced with special strain gaged links. Accelerometers located on the links and stand structure were used to compensate the strain signals for stand movement during the forward-to-reverse thrust transients with a resulting "true" thrust response.

3. Dynamic and Control Parameters - During the engine transient tests, four 8-channel brush-type recorders with selected information were used for "on-line" test monitoring and diagnostics. The parameters monitored are listed in Table 5.

4. Performance Instrumentation - Engine performance instrumentation is shown in Table 6. In addition to the basic engine instrumentation, fan blade position, fan nozzle position, LP and HP rotor speeds were provided from engine control system sensors. Fuel flows were provided from the test cell system. Steady-state thrust readout was provided from a load cell with 25,000 lb forward thrust and 25,000 lb reverse thrust capability. The radial traverse probes (Sta 10 and 15) used $\pm$ 10 psi range transducers. To avoid error due to flow angularity, the probe at the highlight (Sta 10) was aligned with the flow direction.

5. Acoustic - Noise measurements were not of primary importance during these tests, however, far-field noise was recorded during some of the reverse transients with a series of ground microphones spaced every 10^{o} from the inlet axis to 150^{o} on a 45.7 m (150 ft.) radius. Details of the noise acquisition and data reduction techniques are discussed in (3).

DATA REDUCTION - Steady-state reverse thrust performance tests included the direct measurement of the following parameters: engine thrust; fan blade angle; fan and core speeds; fan nozzle position (area); aft fan duct, core inlet, and inlet highlight total pressure radial profiles; fan and engine static pressures; ambient, aft fan duct, and

core inlet air temperature; core engine total and static pressures and temperatures; and ambient conditions of wind velocity, temperature, pressure and relative humidity.

Steady-state reverse thrust data reduction equations are listed in Appendix B. The following parameters were calculated:

1. Corrected engine reverse thrust

2. Corrected fan and core speeds

3. Actual fan blade angle and fan nozzle area

4. Aft fan duct corrected airflow and Mach number

5. Exlet (aft fan duct) and core inlet total pressure recovery

6. Core compressor corrected airflow and pressure ratio, and estimated efficiency

7. Core engine corrected performance parameters

8. Fan airflow, static pressure ratios, and quasi total pressure ratio (at inlet highlight)

9. Exlet, engine, and fan inlet static pressure distributions

Forward-to-reverse thrust transient data reduction consisted of analyzing the data from four recorders (Table 5). Transient data was time synchronized by the power demand signal, and correlated with the steady-state data taken before and after each transient. Calculated values for each successful transient include actual overshoot blade angle, dwell time, actual blade travel time, blade pitch change rate, fan nozzle change rate; thrust response time, flow reattachment time, thrust delay after reattachment, and times to reach final fan speed and final reverse static pressure ratio.

TEST PROCEDURE - Steady-state reverse tests of both the movable flap and the fixed 30° exlets were performed in a similar fashion using the following general procedure:

1. Prior to start-up the desired fan blade angle and fan nozzle area for reverse idle, and other inputs were programmed into the engine digital control.

2. The engine was air motored using dry facility air. At about 3000 RPM core speed, the digital control received sufficient alternator current for regulation and the control signaled the fan blade and fan nozzle to move to the preset reverse values. At about 4000 RPM core speed, the ignitors were activated and ignition was achieved.

3. The engine was accelerated to the reverse idle condition, about 55% fan speed.

4. After the engine was warmed up for about 5 min, conditions were adjusted to the desired settings for reverse data acquisition. Fan blade angle was normally set in the closed direction (see Fig. 8).

Forward-to-reverse thrust transient testing was the last part of the test program because of the inherent greater risk to the engine compared to steady state testing. The sequence of the reverse transients was structured to increase in severity beginning with forward idle-to-reverse idle, and progressing to a forward takeoff-to-reverse thrust transient. Each transient consisted of the following steps:

1. Take forward thrust steady-state data

2. Initiate transient to a reverse set point (blade angle, fan speed and fan nozzle area)

3. Take reverse thrust steady-state data

4. Decrease speed to reverse idle

5. Initiate return transient to forward idle.

All forward-to-reverse thrust transients included an automatic change in fan nozzle area from a forward thrust setting (convergent nozzle) to an open, approximately 30° half-angle flared position to provide an inlet for reverse flow (exlet). Simultaneously, the fan blade pitch was changed on the order of 100° from a forward thrust to reverse thrust setting. The transients were performed from nominal forward idle, approach and takeoff power to various levels of reverse thrust. Other variations included final reverse fan blade angle, blade angle overshoot, and fuel scheduling (fuel interlock setting) during the transient. The maximum attainable fan nozzle and fan blade pitch change rates were used in all the transients.

STEADY-STATE REVERSE THRUST PERFORMANCE

Reverse thrust performance was obtained with the engine at steady-state operating conditions. Covered in this section are reverse starting characteristics; overall, core engine, and fan performance; exlet and core inlet total pressure recovery; engine total pressure and temperature profiles; and the effect of the exlet configuration on steady-state reverse thrust performance. Operational boundary conditions were determined with relatively slow changes in either fan blade angle or fan speed.

REVERSE THRUST STARTING CHARACTERISTICS - Because of the potential reverse "starting" problems (see Introduction), special attention was given to the initial reverse tests of the QCSEE UTW engine. All steady-

state reverse startups were attempted with a preset reverse fan blade angle. Visual observations, as well as thrust readings, indicated reverse thrust was established at the onset of fan rotation for fan blade angles of -91°, -96° and -101°. At a fan blade angle of -86°, the fan appeared to be in a stalled, unstarted condition. The range of fan blade angles where reverse thrust maximizes, as will be discussed later, is -93° to -97°. Consequently, there appears to be a margin of about 5° in starting requirements, β_F = -90° for starting and β_F = -95° for near maximum reverse thrust. Starting characteristics were similar for both the fixed 30° exlet and the movable flap configuration.

OVERALL REVERSE THRUST PERFORMANCE - Variation of corrected reverse thrust with fan speed is shown in Fig. 13 for both the fixed 30° exlet and movable flap configurations. At fan speeds up to 79% of design, thrust peaked at a fan blade angle of -93.6° for the fixed exlet; at higher speeds, and β_F = -93.6°, turbine temperature limits were reached. As fan blade angle was held constant, reverse thrust increased almost linearly with increasing fan speed and began to level off above 80%. Engine core limits were encountered at the higher reverse thrust levels for both exlet configurations. The 27,088 N (6090 lb) reverse thrust goal was attained with the fixed 30° exlet while slightly exceeding the turbine temperature limit. At similar operating conditions and with the movable flap configuration installed, only about 22,240 N (5000 lb) reverse thrust was obtained.

Performance comparisons at constant fan speeds for the two exlet configurations are presented in Fig. 14. At the higher fan speeds, reverse thrust levels of about 26,700 N (6000 lb) were obtained at fan blade angles between -93 and -97° with the fixed exlet (Fig. 14a). Only small gains in reverse thrust with increases in fan speed above 81% are evident as seen by the collapsing speed lines. Maximum reverse thrust was limited by the boundaries indicated on the figure, namely, blade stress at low fan blade angles, core EGT limits near maximum reverse thrust blade angles, and fan speed limits at the higher "off-loaded" blade angles. At the higher fan speeds, the sensitivity was about 890 N (200 lb) of reverse thrust per degree of fan blade angle for both configurations.

At 58% fan speed, a fan blade angle hysteresis check was made with the fixed 30° exlet (Fig. 14a). The data indicated less than 1° of hysteresis with blade angle at this speed. At blade angles from -83 to -91° significantly lower but measurable reverse thrust along with high blade stresses indicated the blades were in a partially stalled mode.

During these tests, consistently higher reverse thrust was obtained with the fixed 30° exlet as compared to the movable flaps at all fan speeds and fan blade angles. In addition, lower blade stresses, lower engine vibrations, and more stable reverse flow were observed. The reverse thrust objective of 27,088 N (6090 lb) could only be achieved with the fixed 30° exlet configuration while slightly exceeding the turbine temperature limit.

EXLET AND CORE INLET TOTAL PRESSURE AND TEMPERATURE CHARACTERISTICS - During reverse operation, air enters the engine from the rear and exits through what is normally the engine inlet. The flow entering the core engine makes a 180° turn and is divided into channels (Sta 21 to 25, Fig. 6) by 6 equally spaced support struts. Rake data at the entrance to the core (Sta 25) were recorded during all steady-state readings. Pressure and temperature profiles were measured during selected operating conditions at the entrance to the fan in reverse (Sta 15) at about a 10 o'clock position and at the fan discharge (Sta 10) at a 6 o'clock position. The "V" shaped gaps between the four nozzle flaps (movable flaps) occur at about the 12, 3, 6 and 9 o'clock positions. Fan and core air flows were calculated from in-duct measurements and the procedures described in Appendix B.

As evidenced, exlet total pressure recovery was significantly improved with the fixed 30° exlet over the movable flaps (Fig. 15). At an aft fan duct Mach number of 0.34, the exlet total pressure recovery was .985 and .948 for the aforementioned configurations. Representative measured pressure and temperature profiles for the fixed and movable flap configurations at comparable fan speeds and fan blade angles are compared in Fig. 16. As can be seen, the pressure loss for the fixed exlet occurs near the outside wall compared to rather uniform losses across the entire duct for the movable flaps. A slight amount of exhaust gas reingestion was observed (Fig. 16a) with measured gas temperatures about 8°K (15°R) above ambient near the inner wall. The traverse data at both the fan entrance and discharge was significantly more oscillatory in nature for the movable flaps indicating more flow turbulence. Static pressure distributions on the exlet surface (see Table 6) indicated flow separation on the inner surface from the sharp aft leading edge to over half the length of the exlet for both configurations. The increased pressure losses with the movable flaps are apparently caused by the sharp edge openings between the four flaps and between the flaps and the outer nacelle and pylon. Blockage or distortion also occurs due to the four flap hinges, actuator rods and pylon.

For the low pressure ratio QCSEE fan (~ 1.08 in reverse), the exlet total pressure recovery is extremely important and, in this case, was the most significant factor causing the relatively low reverse thrust performance of the movable flap configuration.

The core inlet total pressure recovery did not reflect the significant differences observed in average exlet total pressure recovery. This is apparently a result of large pressure losses encountered in turning the flow 180° at the gooseneck entrance to the core, and the fact that most of the core flow is scavenged from the lower recovery flow near the inner wall in the aft fan duct. Core inlet total pressure recovery was similar for both exlet configurations and decreased from about 0.94 to 0.80 as aft fan duct Mach number increased from 0.2 to 0.36. Compressor face pressure profiles at various circumferential locations are compared in Fig. 17. Both configurations had higher pressure recoveries near the inner wall in the core inlet, and in

general, had similar profile shapes. Compressor face temperature profiles at the same conditions as the pressure profiles are shown in Fig. 18. The small amount of hot core gas reingestion measured at the inlet to the fan (Fig. 16) can also be observed at the compressor face. The variation of the average (area weighted) core inlet flow temperature rise with reverse thrust level for both configurations is shown in Fig. 19. At comparable reverse thrust levels, the amount of core exhaust gas reingestion into the compressor inlet appears to be several degrees more for the fixed exlet compared to the movable flap configuration.

CORE ENGINE PERFORMANCE IN REVERSE - Corrected core speed correlates well with corrected fan speed for a given fan blade angle, β_F, for both the fixed 30° exlet and the movable flaps (Fig. 20). Core speed increases rapidly at constant fan speed as fan blade angle is decreased (increasing reverse thrust). Calculated turbine power has similar characteristics. At high corrected core speeds, the core flow approaches a choking condition and remains relatively constant (Fig. 21). The increased turbine work requirement at higher core speeds results in a rapid rise in exhaust gas temperature as fuel is added (Fig. 22) with a notable change in slope at about 80% core speed. The core engine characteristics were similar for both configurations, although a slightly hotter engine exhaust gas temperature of 33°K (60°R) was required to operate at the same corrected core speed with the movable flap configuration.

Calculated specific fuel consumption minimized at a fan blade angle of about -101° for both configurations and was about 10 to 20% lower for the fixed exlet configuration.

FAN PERFORMANCE - Both the fixed and movable flap configurations had about the same calculated corrected flow-fan speed characteristics, Fig. 23. However, actual flows were significantly lower for the movable flap exlet reflecting the lower measured exlet total pressure recoveries (Fig. 6). Air flow was very sensitive to fan blade angle with flow changes as high as 20% measured for 5° blade angle changes near the fan design corrected speed. Fan performance measurements were limited to a total pressure and temperature radial traverse at the entrance to the fan, Sta 15 (Fig. 6) and at the fan discharge, Sta 10. The latter was taken 10.2 cm (4 in) forward of the inlet highlight. Static pressure measurements were also recorded at various stations in the fan flow passage.

Because the fan outlet traverse probe was located beyond the duct, a true total pressure ratio across the fan could not be measured. Consequently, fan rotor tip static pressure ratio which is indicative of total pressure ratio, is presented as a function of corrected rotor flow in Fig. 24. The limited data indicate similar performance for both configurations. At lower rotor flows (lower fan speeds), the effect of blade angle is minimal with a tendency for the data to collapse on one operating line. At the higher flows, and corresponding higher fan speeds, separate operating lines exist as for a family of different fixed-pitch fans. Data obtained with a 20-inch diameter model (15) of

the QCSEE fan show reasonable agreement in the general trends. Typical pressure recovery data obtained with the downstream probe is compared for both configurations in Fig. 25. The fixed exlet configuration had a higher level of total pressure in the exhaust which was concentrated towards the outer wall and neither configuration had outward reverse flow in the center portion. Radial traverse data also indicated significantly more flow instability ahead of and behind the fan with the movable flap configuration; higher blade stresses and engine vibrations were also measured with this configuration. Static wall pressure distributions in the engine inlet (fan discharge) were similar for both exlet configurations.

Although fan performance measurements were limited, it appears that the increased flow distortion and flow turbulence associated with the movable flap configuration, did not significantly affect the fan operating characteristics. These data strongly suggest that the higher thrust level of the fixed 30° exlet is caused primarily by improved exlet total pressure recovery (see earlier discussion) and not by changes in fan performance.

A complete listing of all steady-state performance data acquired for both the fixed 30° exlet and the movable flap configurations is presented in Appendices C and D, respectively.

FORWARD-TO-REVERSE THRUST TRANSIENT PERFORMANCE

A primary requirement of the UTW engine system was the capability of a transient thrust reversal in less than 1.5 sec from approach-to-reverse thrust. To accomplish this, the digital control, on command, synchronized fuel flow changes, fan blade pitch change and the flaring of the fan nozzle movable flaps. Transients were initiated from nominal forward idle, approach and takeoff power to various levels of reverse thrust. Other variations included final reverse blade angle, blade angle overshoot, and fuel scheduling during the transient. A total of nineteen transients were made, all with the movable flaps.

DEFINITIONS OF TRANSIENT TERMS - Definitions and pictorial representation of the terms used in the forward-to-reverse transients are presented in Table 7 and Fig. 26, respectively. For these tests, the primary parameter of interest is the time from the demand for reverse until 80% of the final reverse thrust is achieved. This thrust response time is designated "RESP" . The digital control system was designed such that fuel flow was cut back to an idle setting at the beginning of each transient and held there until the fan blades were well into the transient. Blade position during the transient (fuel interlock setting) was used as the control switch to increase fuel flow. Since the blades reversed such that the angle increased in absolute magnitude (e.g., 0°, -1°, -2° . . . -99°, -100°) during each transient, lower fuel interlock settings (-50°) caused fuel to be increased sooner than higher settings (-90°).

Besides the direct measurement of engine thrust, two other measured parameters, fan blade stress and fan static pressure ratio, were indicative of establishing reverse thrust and are presented. As observed in previous tests (7), fan blade stresses increased substantially during a transient and then suddenly dropped when reverse thrust was established. Also, fan static pressure ratio became zero as the blades stalled, and changed sign as the flow reversed through the engine.

TRANSIENT PERFORMANCE - Summarized in Table 8 is the transient test program. Each transient began at a forward thrust set point F_X, automatically, on command, transitioned to a reverse set point R_X, then a decrease in speed to reverse idle R_1, and finally a transient to forward idle F_1. The nineteen transients are identified as to set point sequence planned (F_X-R_X-R_1-F_1), programmed blade angle overshoot, and the fuel interlock setting angle. Blade angle overshoot was designed for a constant ten degrees beyond final set point for a nominal 0.3 sec time duration. Approximate values of fan blade angle (β_F), fan nozzle area (A18), and fan speed (N_F), are tabulated for the three forward set points, F_1, F_2 and F_3, corresponding to nominal idle, approach and takeoff power settings, respectively. Similar values are listed for the nine reverse set points. Measured β_F, N_F and A18 steady-state reverse values agreed with the scheduled digital control values. Final reverse thrust levels also compared well with previous steady-state thrust data. Transient 13A was performed with an inadvertent control input for final blade angle of -86° rather than -96°, and the engine did not establish reverse thrust because of fan blade stall. This transient is included to help define operational limitations.

After a few transients were performed, it became apparent that fan overspeed would not be a problem. The pre-test concerns of fan overspeed soon gave way to concerns of excessive fan speed decay or undershoot and subsequent long fan spool up times. Attempts to minimize or eliminate this problem were unsuccessful and are discussed later. As a result of this fan speed undershoot, some of the tests planned to investigate ways to minimize thrust response and flow reattachment times by systematic variations in blade pitch change rate and feedback sensitivity were eliminated.

Variation of selected measured parameters during an approach-to-reverse thrust transient without and with fan blade overshoot are presented in Fig. 27 and 28, respectively. A takeoff-to-reverse transient is shown in Fig. 29. During all transients, the fan nozzle movable flaps and the fan blades were moved at their maximum rates. The nozzle flaps (A18 trace) began movement without any measurable lag and moved smoothly and rapidly to the reverse position in 0.7 to 0.8 sec during all the transients. Fan blade movement typically began about 0.1 sec after transient initiation and also moved smoothly and rapidly to the reverse position. However, the blades momentarily overshot the final reverse blade angle by about 3° but damped out to the programmed angle in several cycles. Similarly, 3° of momentary excess overshoot and cyclic

damping occurred when overshoot was programmed (Fig. 28). For the approach and takeoff-to-reverse thrust transients, fan blade pitch change rates ranged from 107 to 120 deg/sec.

The most unexpected transient characteristic observed was the excessive fan speed, N_F, decay or undershoot (Fig. 27 for example) which occurred during the initial portion of each transient. Fan speed dropped approximately 1200 RPM in about 0.7 sec before beginning to recover. The long fan spool-up times resulted in longer than expected times to establish full reverse thrust. Consequently, thrust response time was defined as the time to achieve 80% of final reverse thrust. As can be seen in a typical transient (Fig. 27), all the significant reverse elements (e.g., fan flow was reattached to the fan blades and the fan was not stalled) had been achieved by this time (RESP).

Engine thrust (FG) time histories indicated a brief forward thrust surge of about 14680 N (3300 lb) for 0.25 sec and 2220 N (500 lb) for 0.1 sec as fan blades initially moved open toward stall during the approach and takeoff-to-reverse transients, respectively (Fig. 28 and 29). Subsequently, thrust decayed to zero in about 0.5 sec as the blades rotated through stall. Reverse thrust was established in about 1.5 sec and 1.6 sec for the approach-to-reverse thrust transients with and without overshoot, respectively (Fig. 28 and 27). The shortest thrust response time RESP of 1.1 sec was measured during the takeoff-to-reverse thrust transient (Fig. 29).

For the approach-to-reverse thrust transients, fan blade stress usually peaked after the blade reached the final reverse blade angle (Fig. 27). For the takeoff-to-reverse transient, fan blade stress peaked earlier at about a β_F of -50° at which time the fan was stalled (Fig. 29). In some transients, e.g., Fig. 27, blade stress decrease was a good indicator of the establishment of reverse thrust, as was the case with the Hamilton-Standard Q-Fan demonstrator (7, 8). In other cases, e.g., Fig. 28, blade stress decrease did not correlate well with the establishment of reverse thrust.

Fan tip static pressure ratio, PS2/PS16, decreased slowly throughout the transient as the fan blade moved from forward to reverse blade angles, but lagged, to some degree, measured load cell thrust response times. Tip static pressure ratio could be used in a variable pitch fan engine flight configuration to determine initiation of reverse thrust.

Core speed, N_C, characteristics were similar for all transients, decreasing initially, reaching a minimum in about 0.7 sec and then increasing smoothly to a steady-state value.

The overall sound pressure level, OASPL, at 70° from the inlet (maximum noise location during reverse) at a 46 m (150 ft) radius is shown in the lower curve of these figures. Peak noise levels occur after reverse thrust is established and appear to maximize when final fan speed is reached. Maximum OASPL in reverse is only about 1-2 dB higher than

the maximum OASPL during forward takeoff thrust. However, the perceived noise during reverse is significantly more disturbing because of much higher noise levels in the 1500 to 6000 Hz high annoyance frequency range.

A typical return transient from reverse idle to forward idle is shown in Fig. 30. Blade stresses reached maximum levels at about 0.5 sec into the return at about a $\beta_F = -70^o$. The relatively slow blade travel time of about 1.7 sec in the return direction, compared to about 1.0 sec normally, probably contributed to the relatively high stresses measured.

A summary of all measured and calculated transient performance parameters is tabulated in Appendix E. In Fig. 31 through 36, an attempt was made to isolate the effects of: 1) initial and final fan speed, 2) final blade angle, 3) blade angle overshoot, and 4) fuel scheduling, on thrust response characteristics. As discussed earlier, the fact that large unexpected fan speed decays and subsequent long fan spool up times were encountered during all transients made it difficult to interpret the effect of other parameters. The effect of initial fan speed on RESP and TNF is shown in Fig. 31. As might be expected, thrust response time is shortened when the transient is initiated at higher fan speeds during initial forward thrust operation. As previously discussed, the time to bring fan speed up to 98% of final value, TNF, is greater than RESP and decreases as the initial fan speed is increased.

The effect of final reverse fan speed is shown in Fig. 32 for transients beginning at low forward fan speeds ($N_{FK} = 57\%$). Even though the fan blade pitch change rate was somewhat more rapid during transients to higher reverse fan speeds, the thrust response time was significantly longer due to longer fan spool up times. Final reverse fan speed level had a negligible effect on TNF, BT and RESP if the transient was initiated at high fan speeds, $N_{FK} = 88\%$ (Transient 12 vs 11). To minimize thrust response time, transients should be initiated from relatively high fan speeds in forward thrust and fan speed should be maintained during the transient.

The effect of final reverse fan blade angle on thrust response for transients beginning from approach power is shown in Fig. 33. Data from transient 13A where the blades were in stall is shown for reference. At the same final fan speed, reverse thrust increases as blade angle decreases. Final blade angle had a negligible effect on thrust response time RESP. Longer fan spool up times, TNF, are associated with the higher thrust, more loaded blades ($\beta_F = -100^o$). The time until flow reattaches to the fan blades as determined by the decrease in blade stress (BT + RAT) also increases significantly as the fan blade angle is decreased (increasing reverse thrust).

A fixed 10^o blade angle overshoot of 0.3 sec duration was designed into the control system as a possible solution to anticipated reverse flow starting problems. As discussed earlier, no reverse starting problems were encountered. As shown in Fig. 34, the fixed blade angle overshoot was measured at 13^o and had a negligible effect on thrust

response time. However, the magnitude and duration of high alternating blade stress during the transients was significantly shortened when blade angle overshoot was used (Fig. 35).

The time at which fuel flow was increased after the initial cutback during each transient was controlled by the digital control fuel interlock setting (see Definitions of Transient Terms section). The effects of this parameter are shown in Fig. 36. Variations between -50 and -90° interlock settings did not enhance the unexpected fan speed decay (undershoot) problem as seen at the top of the figure. Neither were thrust response and blade travel times significantly affected. However, time to reach final fan speed, TNF, did appear to minimize at an angle of -60°. Fan speed was near its minimum when the fan blades had rotated to about -50° during the reversals (see Fig. 27, 28 and 29). Increasing fuel flow sooner, (interlock settings less than -50°) might have been beneficial but were not tested because of concerns about possible control system dynamic problems.

Initial design studies of the digital control system indicated possible problems of fan speed overshoot as the fan blades unloaded while changing pitch to the reverse position. To minimize fan overspeed, fuel cutback to flight idle at the onset of all forward-to-reverse transients was incorporated into the digital control logic. No fan overspeed problem was observed in these tests. Apparently the initial fuel cutback was either too abrupt or too severe as unexpected large fan speed decays occurred during the initial portion of the transients and resulted in subsequent long fan spool up times. Within the range tested, rescheduling the time to introduce fuel flow earlier after the initial fuel cutback was unsuccessful in reducing the amount of fan speed decay or length of time to reach final fan speed. No attempt was made to modify the control system logic for these tests. To reduce the time to reach final fan speed in future tests the digital control logic could be modified by controlling fan speed during the transient, delaying slightly the initial fuel cutback, cutting back fuel at a slower rate, or cutting back to a higher fuel flow level above flight idle.

SUMMARY

Steady-state reverse and forward-to-reverse thrust transient performance were obtained with the QCSEE UTW geared variable pitch turbofan engine at the NASA Lewis Research Center. The UTW engine fell short of its reverse thrust goal during its initial testing at the Contractor's facility. It was retested in reverse in its original configuration and with a modified exlet which significantly improved performance. The engine met the steady-state reverse thrust and transient thrust reversal goals. The digital electronic control, variable pitch actuation system, variable pitch composite fan blades and variable fan nozzle operated satisfactorily throughout the tests.

STEADY-STATE REVERSE RESULTS - Reverse thrust performance was obtained with two fan nozzle (exlet) configurations: (a) the QCSEE

4-segment variable area fan nozzle with openings in the flap hinge area and between the flaps when in the reverse position (movable flaps); and (b) a boilerplate continuous, non-gap, 30° half-angle conical exlet (fixed 30° exlet). The steady-state results are summarized below:

1. The reverse thrust goal of 35% of forward static takeoff thrust was attained with the fixed 30° exlet. Reverse thrust with the movable flaps was about 20% less. In order to retain the variable area capability in a flight design and utilize the improved performance concept of the fixed 30° exlet, a new improved movable flap design is required.

2. Lower engine vibrations, lower fan blade stress and more stable flow occurred with the fixed 30° exlet as compared to the movable flaps.

3. No reverse starting problems existed for either configuration.

4. The reverse thrust goal was obtained in a fan blade angle range of about 4°. The operating envelope was bounded by fan blade stress, core exhaust gas temperature, and fan speed limits.

5. Fan performance characteristics did not appear affected by exlet geometry; improved reverse thrust with the fixed 30° exlet appeared to be a direct result of improved exlet total pressure recovery.

6. The core engine characteristics were similar for both configurations, although a slightly hotter engine exhaust gas temperature of about 33°K (60°R), was required to operate at the same corrected core speed with the movable flap configuration. Core engine limits were encountered at the high thrust levels with both configurations.

7. Specific fuel consumption was about 10 to 20% lower for the fixed 30° exlet and optimized at a fan blade angle of about -101° for both configurations.

TRANSIENT RESULTS - Forward-to-reverse thrust transient performance was obtained with the movable flaps only. Automatic thrust reversals were coordinated by the digital control, which on command, synchronized fuel flow changes, fan blade pitch change and the flaring of the fan nozzle movable flaps. Results from the 19 forward-to-reverse thrust transients are summarized below:

1. The transient thrust reversal goal of 1.5 sec from approach-to-reverse thrust was achieved. The takeoff-to-reverse thrust transient was performed in 1.1 sec.

2. Unexpected large fan speed decays and subsequent long fan spool up times were encountered during all transients, apparently due to the early fuel cutback to flight idle as the transient was initiated. To alleviate this problem, the digital control logic could be modified by controlling fan speed during the transient, delaying the initial fuel

cutback, cutting back fuel at a slower rate, or cutting back fuel to a higher level above flight idle.

3. Fan blade pitch change typically began about 0.1 sec after transient initiation, moved smoothly, and momentarily overshot the final reverse blade angle by about 3°, but damped out to the programmed angle in several cycles. Fan blade travel times were on the order of 1.0 sec with measured average pitch change rates from 107 to 120°/sec.

4. Programmed fan blade angle overshoot (10° for 0.3 sec) did not affect thrust response times significantly, but did reduce the magnitude and duration of high blade stress.

5. Fan exhaust nozzle (movable flaps) opened rapidly and smoothly to the reverse setting in about 0.7 to 0.8 sec.

6. A very brief forward thrust surge of 14680 N (3300 lb) and 2220 N (500 lb) occurred as the fan blades initially moved open toward stall during the approach and takeoff-to-reverse transients, respectively.

7. No problems were encountered in establishing reverse thrust, although it took longer times at the higher thrust, more loaded blade angles.

8. Maximum overall sound pressure level was about 1-2 db higher in reverse than at takeoff. However, no anomolies were encountered during the transients.

REFERENCES

1. W. S. Willis "Quiet Clean Short-Haul Experimental Engine (QCSEE)," General Electric Co., Cincinnati, OH, Report No. R79AEG478, August, 1979. (NASA CR 159473, 1979)

2. "Quiet, Powered-Lift Propulsion Conference," NASA 2077, 1978.

3. I. J. Loeffler, N. E. Samanich, and H.E. Bloomer "QCSEE UTW Engine Powered-Lift Acoustic Performance," AIAA-80-1065, June, 1980.

4. H. E. Bloomer, and N. E. Samanich "QCSEE Fan Exhaust Bulk Absorber Treatment Evaluation," AIAA-80-0987, June, 1980.

5. R. E. Neitzel, R. Lee, and A. J. Chamay "QCSEE Task 2: Engine Installation Preliminary Design," General Electric Co., Cincinnati, OH, June, 1973. (NASA CR-134738, 1973)

6. H. E. Helms "Quiet Clean STOL Experimental Engine Study Program. Task I: Parametric Propulsion Systems Studies," Detroit Diesel Allison, Indianapolis, IN, Report No. EDR-7543, September, 1972. (NASA CR-135015, 1972)

7. J. W. Schaefer, D. A. Sagerser and E. G. Stakolich "Dynamics of High-Bypass-Engine Thrust Reversal Using a Variable-Pitch Fan," NASA TM X-3524, 1977.

8. D. C. Reemsnyder and D. A. Sagerser "Effect of Forward Velocity and Crosswind on the Reverse-Thrust Performance of a Variable-Pitch Fan Engine," AIAA Paper No. 79-0105, January, 1979.

9. "Quiet Clean Short-Haul Experimental Engine (QCSEE) - Under the Wing (UTW) Engine Boilerplate Nacelle Test Report, Volume 1: Summary Report," General Electric Co., Cincinnati, OH, Report No. R77AEG2121 - VOL 1, December, 1977. (NASA CR-135249, 1977)

10. "Quiet Clean Short-Haul Experimental Engine (QCSEE) - Under the Wing (UTW) Engine Composite Nacelle Test Report, Volume 1: Summary, Aerodynamic and Mechanical Performance," General Electric Co., Cincinnati, OH, Report No. R78AEG573 - VOL 1, April, 1979. (NASA CR-159471, 1979)

11. W. F. Vier "Quiet Clean Short-Haul Experimental Engine (QCSEE) Test Results from a 14 cm Inlet for a Variable Pitch Fan Thrust Reverser," General Electric Co., Cincinnati, OH, Report No. R75AEG387, December, 1975. (NASA CR-134867, 1975)

12. D. A. Dietrich, T. G. Keith and G. G. Kelm "Aerodynamic Performance of Flared Fan Nozzles Used as Inlets," NASA TM X-3367, 1976.

13. "Quiet Clean Short-Haul Experimental Engine (QCSEE) - Under the Wing (UTW)," General Electric Co., Cincinnati, OH, Final Design Report, June, 1977. (NASA CR-134847, 1977)

14. "Quiet Clean Short-Haul Experimental Engine (QCSEE) - Under the Wing Engine Digital Control System Design Report," General Electric Co., Cincinnati, OH, Report No. R75AEG483, January, 1978. (NASA CR-134920, 1978)

15. R. G. Giffen, R. A. McFalls and B. F. Beacher "QCSEE Aerodynamic and Aeromechanical Performance of a 50.8 cm (20 in) Diameter, 1.34 PR Variable Pitch Fan with Core Flow," General Electric Co., Cincinnati, OH, Report No. R75AEG445, August, 1977. (NASA CR 135017, 1977)

TABLE 1.- QCSEE UTW TECHNICAL GOALS (FOUR-ENGINE, 400,320-N (90,000-lb) THRUST AIRCRAFT)

	Goals
Noise - 152 m (500 ft) sideline	
Approach, EPNdB	95
Takeoff, EPNdB	95
Reverse, PNdB	100
95 EPNdB Contour Area, sq km (sq mile)	1.29 (0.5)
Pollution	EPA 1979 Emission Levels
Installed Thrust	
Forward, N (lb)	77395 (17400)
Reverse (% of takeoff thrust)	35
Specific Fuel Consumption, g/sec-kN (lb/hr-lb)	9.6 (0.34)
Installed Thrust/weight	4.3
Thrust Response	
Approach to Takeoff, sec	1.0
Approach to Reverse, sec	1.5

TABLE 2 - AERODYNAMIC DESIGN PARAMETERS

Total airflow, kg/s (lb/s)	405.5 (894))
Fan tip diameter, cm (in.)	180.3 (71)
Fan tip speed, m/s (ft/s)	289.6 (950)
Bypass ratio	11.8
Fan pressure ratio	1.27
Overall pressure ratio	13.7
Jet velocity (core), m/s (ft/s)	244.7 (803)
Jet velocity (bypass), m/s (ft/s)	204.2 (670)
Gear ratio	2.5

TABLE 3 - ACOUSTIC DESIGN PARAMETERS

[41.2 m/sec (80 knots) aircraft speed; 61 m (200 ft) altitude; takeoff conditions.]

Number of fan blades	18
Fan diameter, cm (in.)	180.4 (71)
Fan pressure ratio	1.27
Fan rpm	3089 (3244 at 100%)
Fan tip speed, m/sec (ft/sec)	289.6 (950)
Number of OGV's	33 (32 + pylon)
Fan weight flow (corrected), kg/sec (lbm/sec)	405.5 (894)
Inlet Mach number (throat)	0.79
Rotor OGV spacing	1.5 rotor tip aerodynamic chords
Fan exhaust area, m^2 (in^2)	1.615 (2504)
Core exhaust area, m^2 (in^2)	0.348 (540)
Gross thrust (SLS uninstalled), kN (lbf)	81.39 (18 300)
Blade passing frequency, Hz	927
Core exhaust flow, kg/sec (lbm/sec)	31.3 (69.1)
Fan exhaust velocity, m/sec (ft/sec)	197.8 (649)
Core exhaust velocity, m/sec (ft/sec)	238.9 (784)
Bypass ratio	12.1
Inlet treatment length/fan diameter	0.74
Van/blade ratio	1.83

TABLE 4 - QCSEE UTW PERFORMANCE

(PREVIOUSLY REPORTED)

Noise - 152 m (500 ft) sideline

Approach - 98.5 EPNdB
Takeoff - 99.7 EPNdB
Reverse - 106.4 PNdB @ 27% of takeoff thrust
95 EPNdB Contour Area - 2.59 sq km (1.0 sq mile)

Pollution

Met EPA 1979 Emission Levels

Installed thrust

Forward - 77, 395 N (17,400 lb)
Reverse - 27% of takeoff thrust

Specific Fuel Consumption

9.6 g/sec-kN (0.34 lb/hr-lb) - sea level static

Installed Thrust-to-Weight

4.15

Thrust Response

Approach-to-takeoff - not attempted

TABLE 5 - SANBORN REQUIREMENTS FOR

TRANSIENT TESTING

Ch. No.	Parameter
	SANBORN A
*1	Power Demand (PD) or Mode
2	A18 TMC
3	Nozzle Area, A18
4	Core Speed N2
5	Fan Speed NIF
6	Thrust, FG (load cell)
7	Calc T41, T41C
8	Pressure Ratio, PS3/pto
	SANBORN B
*1	Power Demand or Mode
2	WF TMC (fuel flow - torque motor current)
3	WF (fuel flow)
4	FMP (fuel manifold press)
5	XM11 (throat Mach No.)
6	PLA (power lever angle)
7	VSV (variable stator vane)
8	Selectable Channel
	SANBORN C
*1	Power Demand or Mode
2	βf TMC
3	Fan Pitch Angle, βf
4	βf open pressure
5	βf close pressure
6	Blade Strain
7	Blade Strain
8	Blade Strain
	SANBORN D
1	Thrust FG (load cell)
2	Link 1 Strain
3	Link 2 Strain
4	Link Accelerometer
5	Load Cell Accelerometer
6	Link AVG Compensated
7	Load Cell Compensated
8	True Thrust Transient

*Power Demand (PD) for Forward Transients and (Mode) for Reverse Transients

TABLE 6 - ENGINE PERFORMANCE INSTRUMENTATION

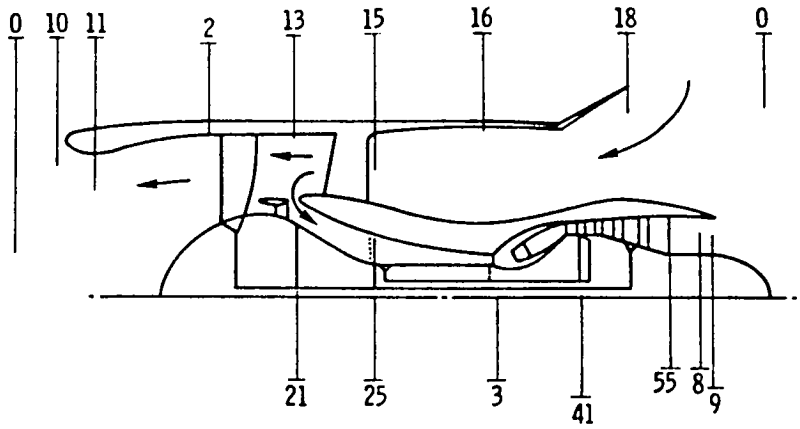

Inlet Highlight (Sta 10)

Pt and Tt radial traverse @ 180°

QCSEE Inlet (Highlight to compressor face)

2 axial rows of 16 wall statics @ 180° and 270°
1 circumferential row of 8 wall statics at throat (Sta 11)

Fan Frame (~ Sta 13)

19 statics on outer wall

Bypass Duct Fan Inlet (Sta 15)

Pt and Tt radial traverse @ 283°

Fan Duct Measuring Station (Sta 16)

4 outer wall and 4 inner wall statics

Fan Duct Entrance

2 statics on outer wall

30° Exlet

1 axial row of 9 wall statics

Movable Flaps

4 axial rows of 7 wall statics each of flap #3

Core Entrance Island (~ Sta 21)

5 island wall statics
5 core 06V vane statics
2 hub wall statics
2 3-element Pt rakes @ 170° and 350°

Core Entrance Splitter Lip (~ Sta 21)

4 wall statics

Core Entrance Gooseneck (Sta 21 to 25)

6 inner wall statics

Compressor Face (Sta 25)

4 outer and 4 inner wall statics
6 5-element Pt rakes @ 16, 82, 105, 145, 225, 282°
6 5-element Tt rakes @ 16, 82, 105, 145, 225, 282°

Core Compressor Discharge (Sta 3)

1 T3 probe
1 PS3 probe

LP Turbine Frame Discharge (Sta 55)

1 5-element Tt rake

TABLE 7 - FORWARD-TO-REVERSE THRUST TRANSIENT TERMS

BT	Blade travel time, s; time from request to reverse engine thrust until fan blade initially reaches within 1° of overshoot blade angle
DELAY	Thrust delay after reattachment, s; time from flow reattachment to fan blade (blade stresses drop below reference value) until 80% of final reverse thrust is achieved.
DOV	Number of degrees of overshoot beyond the final reverse blade angle, deg.
DWELL	Time that fan blade is held at the overshoot blade angle, s.
NFOS	Max fan speed above reverse set point, RPM
NFUS	Min fan speed blow forward set point, RPM
OBA	Overshoot blade angle, deg.
PCR	Pitch change rate; average blade travel rate, $\frac{OBA - \beta_{Fi}}{BT}$, deg/s
PD	Power demand, %
RAT	Flow reattachment time, s; time when fan blade intially reaches within 1° of overshoot blade angle until fan comes out of stall (blade stresses drop below reference value)
RESP	Thrust response time, s; time from request to reverse engine thrust until 80% of final reverse thrust is achieved (RESP = BT + RAT + DELAY)
TA18	Time from request to reverse engine thrust until A18 opens to 98% reverse setting
TNF	Time from request to reverse engine thrust 98% of final fan speed is achieved, s.
TSP	Time from request to reverse engine thrust until 98% of final reverse static pressure ratio PS2/PS16 is obtained, s.

TABLE 8 - SUMMARY OF FORWARD-TO-REVERSE TRANSIENTS

Number	Transient	Blade Overshoot	Fuel Interlock Setting
1	F1-R1-F1	No	-90°
2	F1-R1-F1	No	-90°
3	F1-R2-R1-F1	No	-90°
4	F1-R3-R1-F1	No	-90°
5	F1-R4-R1-F1	No	-90°
6	F2-R4-R1-F1	No	-90°
7	F2-R4-R1-F1	No	-70°
8	F2-R4-R1-F1	No	-60°
9	F2-R4-R1-F1	Yes 115/105	-70°
10	F2-R5-R1-F1	No	-70°
11	F2-R6-R1-F1	No	-70°
12	F2-R7-R1-F1	No	-70°
13	F3-R4-R1-F1	No	-70°
14	F2-R8-R1-F1	Yes 110/100	-70°
15	F2-R8-R1-F1	No	-70°
16	F2-R4-R1-F1	No	-50°
17	F2-R4-R1-F1	Yes 115/105	-50°
*18	F2-R4-R1-F1	Yes 115/105	-50°
**13A	F2-R9-R1-F1	Yes 100/90	-70°

*Blades stopped at -57°. Lost hydraulic pressure. First fully automatic transient.

**Blades stalled.

Forward Set Points

	β (Panel)	A18 (Panel)	~ Fan Speed rpm (%)
F1	+ 2.4	2480	1800 (56)
F2	0	2900	2850 (88)
F3	- 10.0°	2350	3073 (95)

Reverse Set Points

	β (Panel)	A18 (Panel)	~ Fan Speed rpm (%)
R1	-105	3900	1806 (56)
R2	-105	3900	2083 (64)
R3	-105	3900	2637 (81)
R4	-105	3900	2894 (89)
R5	-115	3900	2890 (89)
R6	-110	3900	1800 (56)
R7	-110	3900	2886 (89)
R8	-100	3900	2624 (81)
R9	- 90	3900	2624 (81)

APPENDIX A

Symbols

A18	bypass nozzle lip area
A_{te}/A_D	exlet trailing edge to fan duct area ratio
D_F	inlet diameter at fan face
D_{HL}	inlet highlight diameter
D_t	inlet throat diameter
EGT	exhaust gas temperature, °R; (LPT Discharge Sta. 55)
FGK	ave. corrected engine reverse thrust, lb
FG8	est. core thrust, lb
HUM	grains of water per lb of dry air
L	inlet length from highlight to diffuser exit (fan face)
M_D	aft fan duct Mach number
N_C	core speed, rpm
N_{CK}	corrected core speed $(N_C/\sqrt{\theta_{25}})$, %
N_F	fan speed, rpm
N_{FK}	corrected fan speed $(N_F/\sqrt{\theta_0})$, %
OL	operating line
P_S	local static pressure
P_{S2}/P_{S13}	fan tip static-pressure ratio (reverse)
P_{T3}/P_{T25}	HP core compressor total pressure ratio
P_T	local total pressure
P_{T0}	ambient pressure
P_{T2}/P_{T0}	fan outlet total pressure (at fan face)
P_{T2}/P_{T15}	fan pressure ratio (reverse)
P_{T15}/P_{T0}	exlet total-pressure recovery
P_{T25}/P_{T0}	core compressor inlet total-pressure recovery (including exlet)
R_F	fan radius at leading edge
SFCK	corrected specific fuel consumption (lb/hr)/lb
SLS	sea-level static
SS	steady state

TO	takeoff
T_0	ambient temperature, °R
T25	core compressor inlet total temp., °R
T41K	corrected HPT rotor inlet total temperature, °R (T3, PS3, W_F digital control)
T55K	corrected exhaust gas temperature, °R
W11K	corrected fan rotor flow, lb/s
W15K	corrected aft fan duct flow, lb/s; (total fan plus core inlet flow)
W25K	corrected core compressor inlet flow, lb/s
x	axial distance from inlet highlight
β_F	fan blade angle, angle from design forward blade angle, deg
δ	ratio of total pressure to standard sea-level pressure
θ	ratio of total temperature to standard sea-level temperature

APPENDIX B

Steady-State Reverse Thrust Calculations

1. Corrected thrust, FGK

$$FGK = \frac{F_G}{\delta o}$$

2. Weight flow

$$W = 2.0519 \times C_D \times A \times \frac{P_T}{\sqrt{T_T}} \times \sqrt{\left(\frac{Ps}{P_T}\right)^{1.427} - \left(\frac{Ps}{P_T}\right)^{1.7135}}$$

For Aft Fan Duct Flow, W_{15}

$C_D = 0.98$

$A_{16} = 3262.8\ in^2$

$P_T = P_{T15}$, psia

$T_T = T_0\ ^oR$

$Ps = P_{S16}$, psia

For Core Flow, W_{25}

$C_D = 0.70$

$A_{25} = 328.68\ in^2$

$P_T = P_{T25}$, psia

$T_T = T_{25}$, ^oR

P_{S25} = psia

For Rotor Flow, $W_{11} = W_{15} - W_{25}$

3. Corrected weight flow

$$WxxK = \frac{Wxx \times \sqrt{\theta xx}}{\delta xx} \times \left(1 + .34\ \frac{HUM}{7000}\right)$$

4. Aft fan duct Mach number, M_D

$$M_D = 2.2319 \times \left[\left(\frac{Ps}{P_T}\right)^{-.2865} - 1.0\right]^{\frac{1}{2}}$$

5. Core compressor pressure ratio, P_{T3}/P_{T25}

$$\frac{P_{T3}}{P_{T25}} = \frac{1.0193\ P_{S3} - 2.05}{P_{T25}}$$

6. Corrected fan speed, N_{FK}

$$N_{FK} = \frac{N_F \left(1 - .26\ \frac{Hum}{7000}\right) \times 100}{3244.1 \times \sqrt{\theta_{15}}}$$

7. Corrected core speed, N_{CK}

$$N_{CK} = \frac{N_C \left(1 - .26\ \frac{Hum}{7000}\right) \times 100}{N_{CDES} \times \sqrt{\theta_{25}}}$$

APPENDIX C - STEADY-STATE REVERSE PERFORMANCE 30° HALF-ANGLE CONICAL EXLET

		ENGINE					CORE			FAN DUCT EXLET			FAN ROTOR INLET		
Rdg.	β_F deg.	NFK %	NFK rpm	NCK %	FGK lbs	T41K % des.	T55K % des.	PT3/PT25 --	PT25/PTO --	W25K % des.	MD --	PT15/PTO --	W15K lbs/s	W11K lbs/s	PS2/PS13 --	PS2/PTO --
1011	-106.3	61.2	1982	76.2	-2264	66.3	75.3	5.50	.934	51.1	.198	.994	367.6	336.4	1.043	.981
1013	-106.2	82.7	2681	82.4	-3687	75.4	81.2	8.22	.897	72.9	.258	.992	470.3	427.5	1.075	.967
1014	-106.2	95.3	3088	84.9	-4065	82.1	86.6	9.70	.877	81.1	.274	.990	497.5	450.8	1.085	.955
1018	-101.2	59.3	1921	78.9	-3038	68.1	75.5	6.41	.912	60.0	.228	.992	419.0	383.2	1.056	.978
1020	-101.2	82.2	2664	85.9	-5213	84.1	88.6	10.28	.843	86.8	.313	.989	560.0	512.4	1.125	.962
1021	-101.2	88.3	2863	87.4	-5400	88.6	93.1	11.10	.833	90.5	.320	.988	571.2	521.6	1.139	.954
1030	-101.2	56.8	1845	78.4	-2796	67.8	75.1	6.17	.914						1.058	.981
1031	-101.2	64.1	2079	80.8	-3440	71.4	78.1	7.25	.895						1.074	.974
1032	-101.2	82.2	2667	86.0	-5150	84.8	89.4	10.28	.841	86.9					1.125	.961
1033	-101.2	88.1	2856	87.4	-5375	89.1	93.4	11.10	.832	91.4					1.142	.956
1034	-101.3	95.1	3085	88.5	-5420	91.7	95.6	11.71	.830	92.9					1.147	.952
1035	- 99.0	95.1	3084	89.6	-5650	95.2	99.1	12.12	.822	95.8					1.159	.952
1036	- 95.9	56.6	1837	81.2	-3341	71.3	77.8	7.43	.882	68.2	.264	.991	480.9	441.6	1.070	.976
1037	- 95.9	64.4	2090	84.1	-4520	79.8	83.5	9.05	.847						1.094	.969
1038	- 95.8	81.9	2657	91.0	-5897	99.0	103.1	12.56	.790	98.5					1.168	.949
1039	- 95.8	88.2	2861	94.2	-6000	104.5	109.3	13.22	.783	99.2					1.187	.949
1040	- 94.7	81.7	2651	92.2	-6075	100.5	104.3	12.72	.784	98.8					1.169	.947
1041	- 93.6	81.7	2628	93.6	-5973	103.5	107.1	13.08	.774	98.9					1.171	.948
1042	- 98.5	81.7	2652	87.8	-5573	88.0	93.1		.817	92.2					1.141	.952
1043	- 96.4	81.8	2654	89.8	-5999	94.4	98.4	12.17	.797	96.2					1.164	.952
1044	- 91.3	57.2	1851	83.1	-3548	74.6	80.4	8.47	.857	77.1	.282	.989	512.6	467.3	1.071	.976
1045	- 91.2	64.5	2090	85.8	-4472	81.6	85.9		.827						1.092	.973
1046	- 93.6	57.4	1858	82.8	-3788	74.0	79.1		.862						1.076	.974
1047	- 93.6	64.3	2084	85.5	-4497	81.3	85.3		.830						1.100	.970
1048	- 93.6	79.1	2566	94.1	-6194	103.4	107.4	13.11	.772	99.1					1.165	.956
1049	-106.4	57.3	1860	75.1	-2031	64.5	74.6		.943						1.040	.985
1050	-106.4	64.4	2087	77.6	-2635	66.6	75.2		.929						1.047	.979
1051	-106.4	81.8	2658	82.1	-3703	74.5	80.5		.896						1.075	.967
1052	-106.4	87.9	2848	83.5	-3930	78.3	83.2		.889						1.081	.963
1053	-106.4	95.4	3095	85.1	-3932	81.6	86.2		.877						1.086	.958
1054	-106.5	88.0	2854	83.0	-3720	77.0	82.7	7.59	.894						1.076	.965
1055	-106.5	79.2	2569	80.9	-3444	72.7	80.1	6.67	.908						1.063	.970
1056	- 93.6	56.4	1829	82.3	-3696	73.4	79.5	7.94	.870	72.5	.273	.989	494.6	453.4	1.071	.974
1057	- 94.2	56.4	1828	82.0	-3420	72.8	79.2	6.74	.874						1.072	.976
1058	- 94.2	64.4	2088	84.9	-4663	80.2	85.0	7.96	.835						1.096	.967
1059	- 94.2	82.8	2688	94.2	-6160	104.1	107.6	13.14	.779	99.8					1.179	.952

APPENDIX D - STEADY-STATE REVERSE PERFORMANCE MOVABLE FLAPS

	ENGINE					CORE					FAN DUCT EXLET			FAN ROTOR INLET		
Rdg.	β_F deg.	NFK %	NFK rpm	NCK %	FGK lbs	T41K % des	T55K % des	PT3/PT25 --	PT25/PTO --	W25K % des	MD --	PT15/PTO --	W15K lbs/s	W11K lbs/s	PS2/PS13 --	PS2/PTO --
916	-106.1	52.2	1692	73.2	-1684	66.5	74.8	4.64	.947						1.039	.983
917	-106.2	55.1	1783	74.0	-1714	66.8	74.4	4.65							1.041	.981
918	-106.2	54.9	1782	73.7	-1657	65.6	69.9	4.87	.939	47.2	.195	.985	361.0	332.9	1.042	.982
919	-106.2	54.8	1779	74.0	-1650	64.2	74.2	4.88	.940	48.2	.200	.987	370.0	341.5	1.038	.980
920	-106.4	62.1	2014	76.4	-2062	66.4	75.2	5.67	.928	55.4	.213	.982	393.3	360.0	1.048	.975
921	-106.5	78.9	2560	81.1	-3150	76.9	81.2	7.66	.891	70.0	.265	.972	473.4	431.7	1.078	.963
922	-106.4	94.2	3055	84.3	-3572	82.2	88.0	9.69	.860	80.6	.275	.963	499.6	453.6	1.103	.954
923	-106.4	82.2	2667	81.4	-3150	77.7	82.2	8.04	.880	68.0	.262	.971	476.6	437.0	1.080	.962
924	-106.5	54.5	1762	73.5	-1522	64.6	74.9	4.48							1.036	.981
925	-101.3	55.2	1790	77.4	-2029	68.2	74.2	5.47	.909						1.055	.976
926	-101.3	62.5	2027	79.9	-2672	73.1	77.8	7.14	.886	63.7	.247	.970	460.5	423.0	1.072	.969
927	-101.3	80.6	2615	85.2	-4308	83.8	90.9	10.20	.831	87.5	.311	.952	557.4	508.8	1.128	.953
928	-101.3	85.5	2774	86.7	-4636	87.5	93.7	11.01	.814	89.1					1.147	.949
929	-101.3	93.4	3029	88.6	-4711	93.6	98.9	11.95	.802	92.6	.335	.950	592.9	543.0	1.165	.943
930	-101.3	85.4	2769	85.9	-4547	86.3	92.2	10.72	.817	85.8					1.140	.952
931	-101.3	54.6	1772	76.9	-2215	66.7	74.8	5.25	.898						1.055	.977
932	- 96.1	54.7	1773	79.9	-2617	69.3	76.5	7.14	.878	61.7	.260	.971	473.2	438.0	1.065	.971
933	- 96.1	62.2	2016	82.6	-3268	78.1	81.8	8.60	.848	74.2	.284	.959	512.8	471.0	1.085	.961
934	- 96.1	79.8	2587	90.0	-4939	97.7	99.0	12.14	.779	96.3					1.155	.942
935	-111.3	60.2	1951	72.9	-1400	63.9	73.7	4.34							1.029	.981
936	-111.2	79.0	2562	78.2	-2068	68.5	76.5	5.97							1.048	.971
937	-106.5	79.1	2565	80.9	-2741	75.7	80.0	6.77							1.070	.962
938	-101.3	79.2	2570	84.4	-3970	83.5	88.0	7.97							1.113	.955
939	-104.0	78.9	2559	82.7	-3615	80.2	82.8	7.35							1.095	.960
940	-106.5	79.0	2564	81.0	-2962	76.3	80.7	6.85							1.076	.964
941	-111.4	79.1	2565	78.2	-1920	69.1	77.3	5.86							1.045	.970
942	-115.1	79.2	2568	76.2	-1250	68.3	75.9	5.30							1.025	.974
943	-111.2	79.0	2562	78.0	-1898	70.6	76.7	5.81							1.042	.971
944	- 91.4	54.9	1780	81.2	-2097	71.2	77.2	6.52							1.061	.971
945	- 91.4	62.3	2020	83.5	-2762	79.8	81.7	7.46							1.078	.967

NASA-C-8010 (10-24-51)

APPENDIX E - TRANSIENT PERFORMANCE

			ENGINE						THRUST				BLADE DYNAMICS						BLADE STRESS		
No	PD %		A18 in^2	TA18 s	NCK %	NFK RPM	TNF s	NFUS & NFOS RPM	PS2/PS16 --	TSP s	FGK lbs	RESP s	DELAY s	β_F Deg	DOV Deg	OBA Deg	DWELL s	BT s	PCR Deg/s	BT + RAT s	RAT s	$\sigma_{B\ MAX}$ ± KPSI
1	45.2		2480	.7	75.4	57.0	1.7	1020	.937	1.90	4579	1.8	- .1	+ 5.2	1.0	-102.6	.07	1.30	82.9	1.90	.60	10.0
	45.0		3906		77.6	56.6			1.035		-2173			-101.6								
2	45.2		2480	.7	75.8	57.0	1.6	1020	.938	1.90	4644	1.8	- .1	+ 5.0	1.0	-102.4	.12	1.20	89.5	1.90	.70	10.5
	45.0		3906		78.1	56.7			1.037		-2359			-101.4								
3	45.2		2478	.7	75.6	56.9	2.8	1120	.940	1.80	4650	2.0	+ .25	+ 5.1	2.0	-103.3	.15	1.20	91.2	1.75	.60	10.0
	54.1		3906		81.3	65.4			1.049		-3074			-101.4								
4	45.2		2479	.7	75.4	56.8	4.1	1100	.941	3.5	4517	3.0	1.55	+ 5.1	3.0	-104.7	.15	.95	116.6	1.45	.50	8.0
	72.7		3904		85.9	82.2			1.069		-4444			-101.7								
5	45.2		2479	.7	75.4	56.5	5.0	1100	.940	3.8	4546	3.5	2.1	+ 5.3	3.0	-104.6	.15	.90	123.2	1.40	.50	11.0
	81.1		3904		88.4	90.5			1.075		-4626			-101.6								
6	79.8		2904	.7	82.7	88.5	3.9	1600	.865	2.9	10077	1.4	-2.0	+ 2.6	3.0	-104.4	.2	.90	120	3.4	2.5	7.5
	81.2		3902		88.4	89.9			1.072		-4474			-101.4								
7	79.8		2904	.7	82.8	88.2	3.2	1600	.858	2.5	10662	1.2	-1.5	+ 2.3	3.0	-104.4	.2	.90	119.7	2.7	1.8	9.0
	81.2		3903		88.4	89.8			1.074		-4506			-101.4								
8	79.8		2904	.7	83.0	88.3	3.1	1600	.855	2.3	10683	1.2	-1.5	+ 2.5	3.0	-104.7	.15	.90	119.1	2.7	1.8	9.0
	81.3		3899		88.1	89.7			1.072		-4695			-101.7								
9	79.8		2903	.8	82.8	88.1	2.6	1650	.858	2.2	10660	1.5	- .6	+ 2.5	13.0	-114.9	.5	1.0	121.4	2.1	1.1	7.0
	81.3		3902		87.2	89.7			1.065		-4256			-101.9								
10	79.7		2904	.8	82.9	88.1	1.9	1600			10750	1.5	- .1	+ 2.4	4.0	-115.7	.15	1.0	119.1	1.6	.6	8.0
	81.3		3906		80.9	89.7		3000			-2350			-111.7								
11	79.8		2904	.7	72.9	88.1	2.3	1650			10700	1.1	- .05	+ 2.5	3.0	-109.7	.05	1.0	112.2	1.15	.15	8.0
	44.8		3905		74.5	55.4					-1530			-106.7								
12	79.7		2904	.7	83.0	88.2	2.3	1640	.855	1.6	10768	1.2	- .7	+ 2.5	3.0	-109.7	.05	1.05	106.9	1.90	.85	8.0
	81.3		3903		83.7	89.8		2960	1.043		-3400			-106.7								
13	87.6		2350	.7	89.4	95.5	2.1	1950	.736	1.5	17136	1.1	+ .1	- 7.2	3.0	-104.5	.05	.92	106.8	1.0	.08	11.0
	81.2		3903		87.6	89.5			1.074		-4607			-101.5								
14	80.4		2903	.7	82.9	88.9	3.5	1650	.861	2.1	10630	1.5	+ .4	+ 3.1	13.0	-109.8	0.35	1.00	117.9	1.10	.1	5.6
	72.7		3902		89.9	81.2			1.074		-4940			-96.8								
15	80.4		2904	.75	83.0	88.5	3.5	1650	.860	1.7	10632	1.6	- .05	+ 3.1	3.0	- 99.8	.1	0.95	108.3	1.65	.70	9.0
	72.7		3902		90.6	81.2			1.075		-4945			-96.8								
16			2902	.7	82.6	88.9	3.2	1680	.861	1.8	10083	1.3	-1.2	+ 3.1	3.0	-104.8	.1	1.0	108.9	2.5	1.5	7.0
			3902		87.0	90.4			1.073		-4331			-101.8								
17			2902	.8	82.7	88.7	2.2	1700	.863	1.8	10375	1.5	+ .35	+ 3.4	13.0	-114.8	.47	1.1	111.1	1.15	.05	7.0
			3903		86.4	90.3			1.069		-4292			-101.8								
*18			2904	.93	82.8	88.9	4.1	1750	.864	1.8	10421	∞		+ 3.1	0	- 53.4	0	.62	91.0	stall ∞	∞	10.0
			3900								+ 607			-53.4								
			2900		77.2	42.6			.997		+ 607			-53.4								
13A			2902	.8	82.7	88.0	3.5	1650	.861	1.9	10765	stall		+ 3.0	13.0	-100	.4	.93		stall ∞	∞	11.0
			3900		82.3	80.9		2750	1.040		0			-87.0								

*DURING TRANSIENT, FAN BLADES STOPPED AT -53.4° AND REMAINED IN STALL DUE TO LOSS OF HYDRAULIC PRESSURE

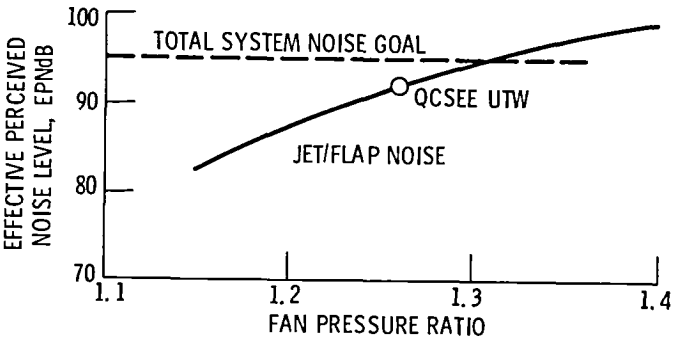

Figure 1. - Effect of jet flap noise on fan pressure ratio selection.

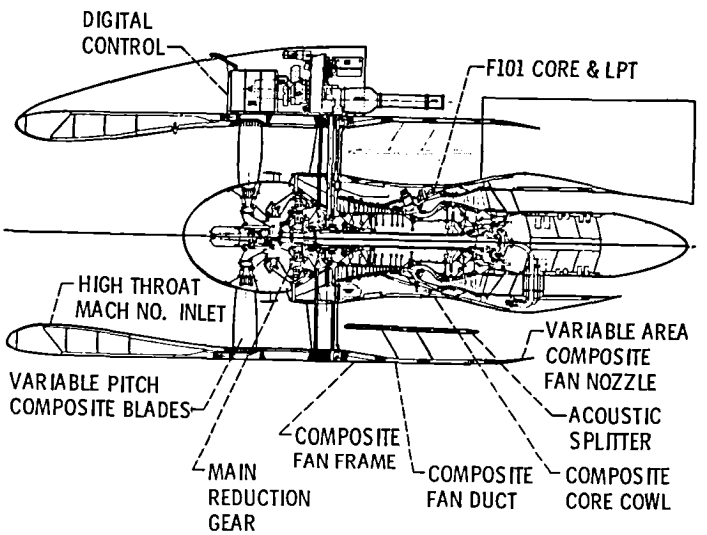

Figure 2. - UTW Engine cross section.

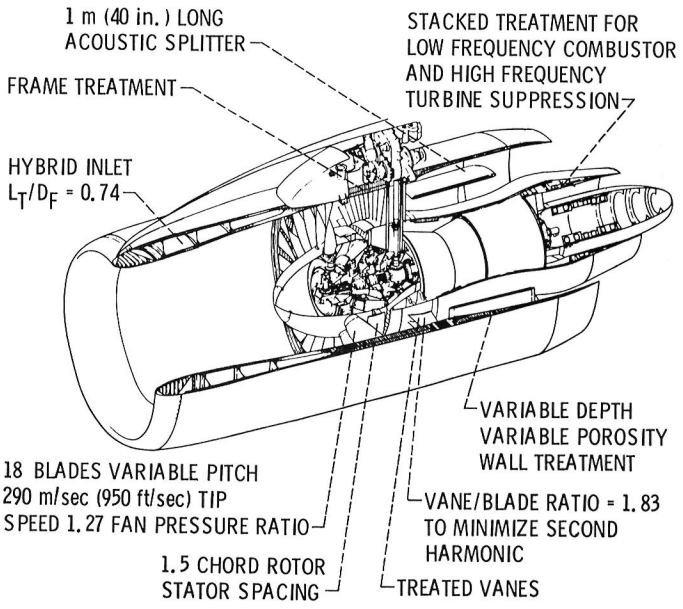

Figure 3. - Acoustic design features of QCSEE UTW engine.

Figure 4. - Engine test stand - front view.

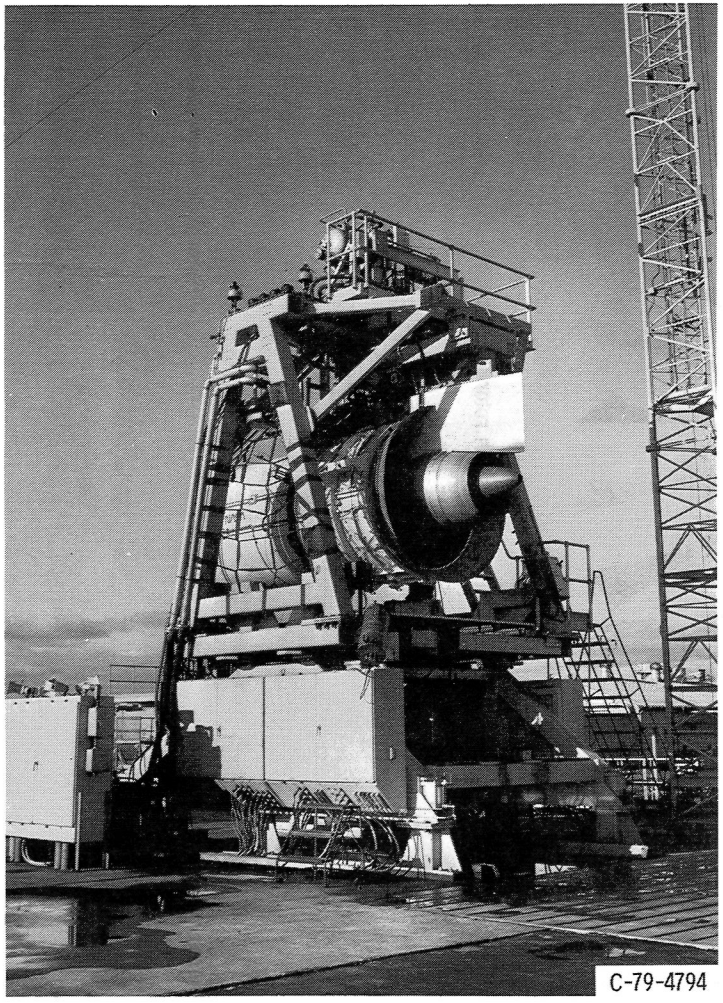

Figure 5. - Engine test stand-aft view.

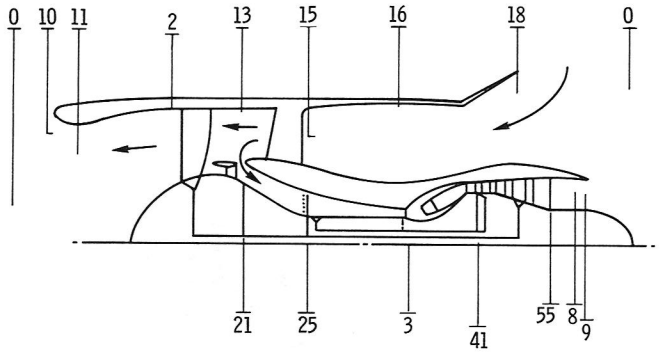

STATION

0	FREE STREAM AIR CONDITIONS
10	RADIAL TRAVERSE (FAN DISCHARGE P_T, 4" FORWARD OF INLET HIGHLIGHT)
11	INLET THROAT (FAN DISCHARGE, P_S)
2	FAN FRONT FACE (FAN DISCHARGE, P_S)
21	FAN HUB DISCHARGE (INLET TO GOOSENECK)
25	HP COMPRESSOR INLET (RADIAL TOTAL PRESS & TEMP RAKES)
3	HP COMPRESSOR DISCHARGE (STATOR EXIT)
41	HP TURBINE ROTOR INLET
55	LP TURBINE FRAME DISCHARGE, EGT
8	PRIMARY EXHAUST NOZZLE THROAT
9	PRIMARY EXHAUST NOZZLE DISCHARGE
13	ROTOR INLET - FAN ROTOR TIP INLET P_S
15	BYPASS DUCT (FAN INLET - RADIAL TRAVERSE AT BYPASS OGV TRAILING EDGE, P_T, T_T)
16	BYPASS DUCT - (STATION 225 - FAN INLET FLOW MEASUREMENT P_S)
18	BYPASS EXHAUST NOZZLE DISCHARGE (EXLET TRAILING EDGE)

Figure 6. - Station designations - reverse thrust configuration.

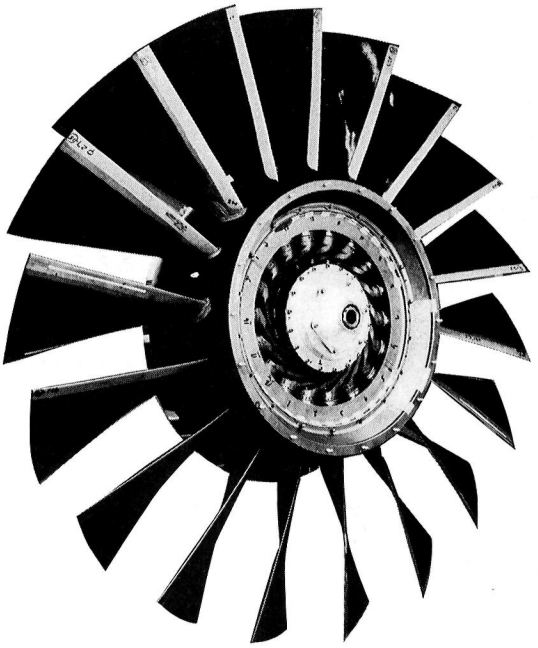

Figure 7. - UTW fan rotor.

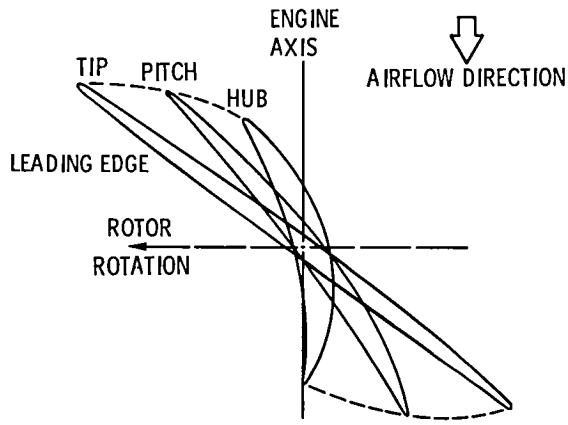

(a) Forward-mode operation.

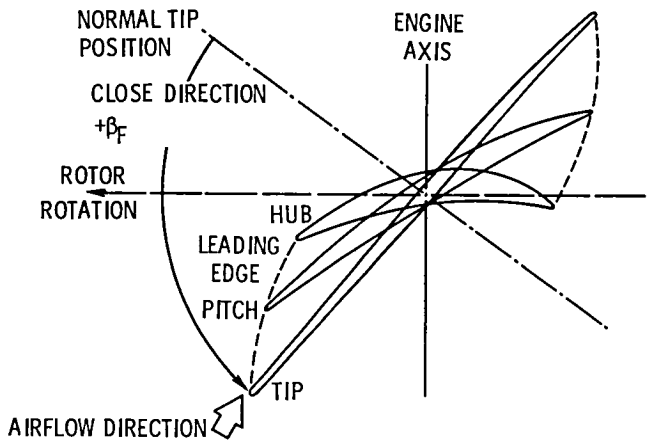

(b) Reverse through flat pitch operation.

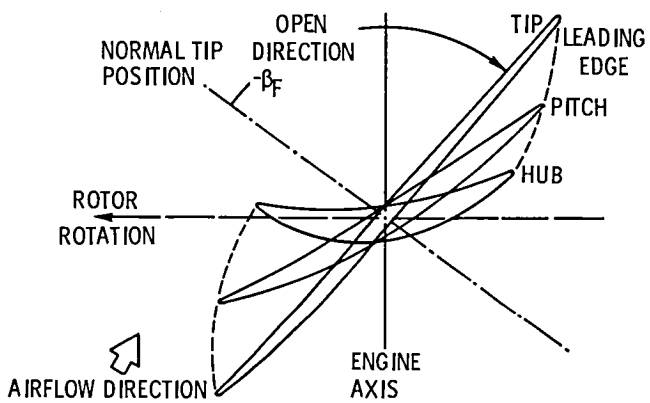

(c) Reverse through stall operation.

Figure 8. - UTW fan rotor blade.

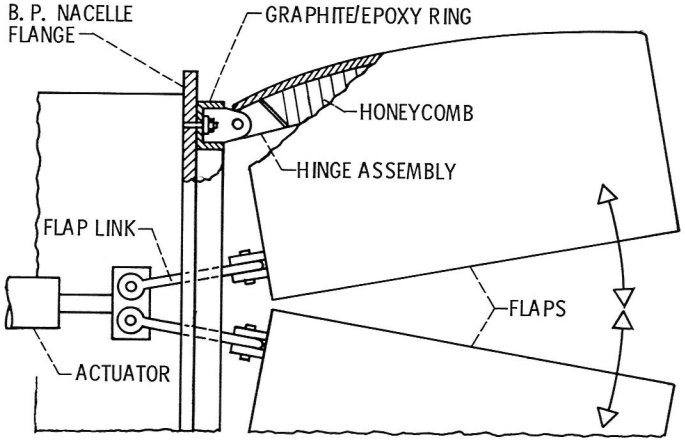

Figure 9. - Schematic-movable flaps.

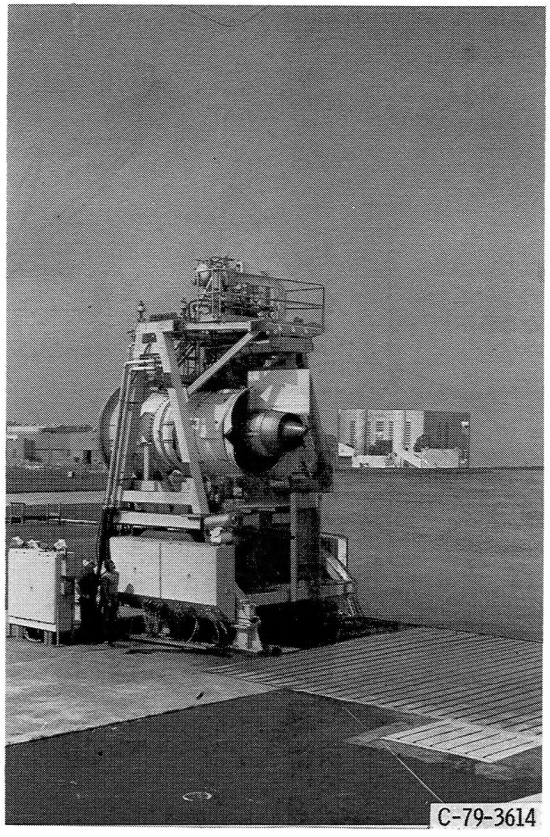

Figure 10. - 3/4 Aft view of movable flap configuration "on-test."

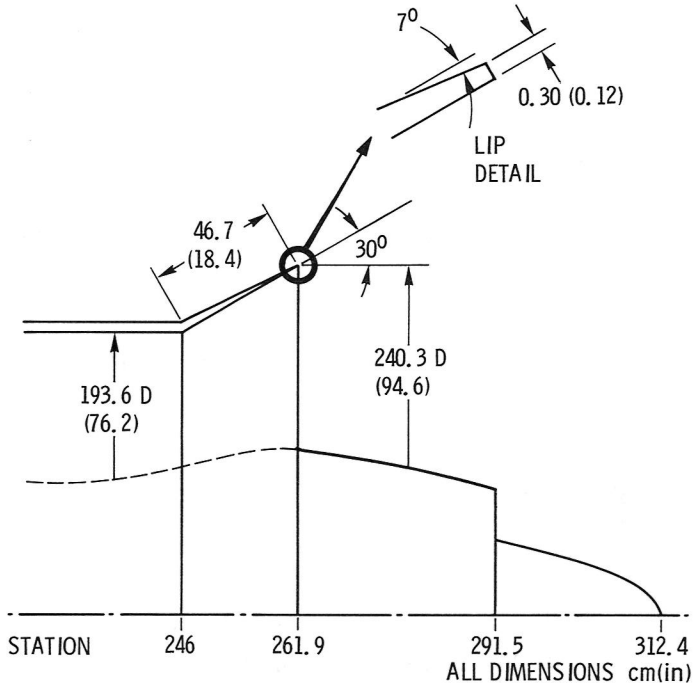

Figure 11. - Schematic-fixed 30° exlet.

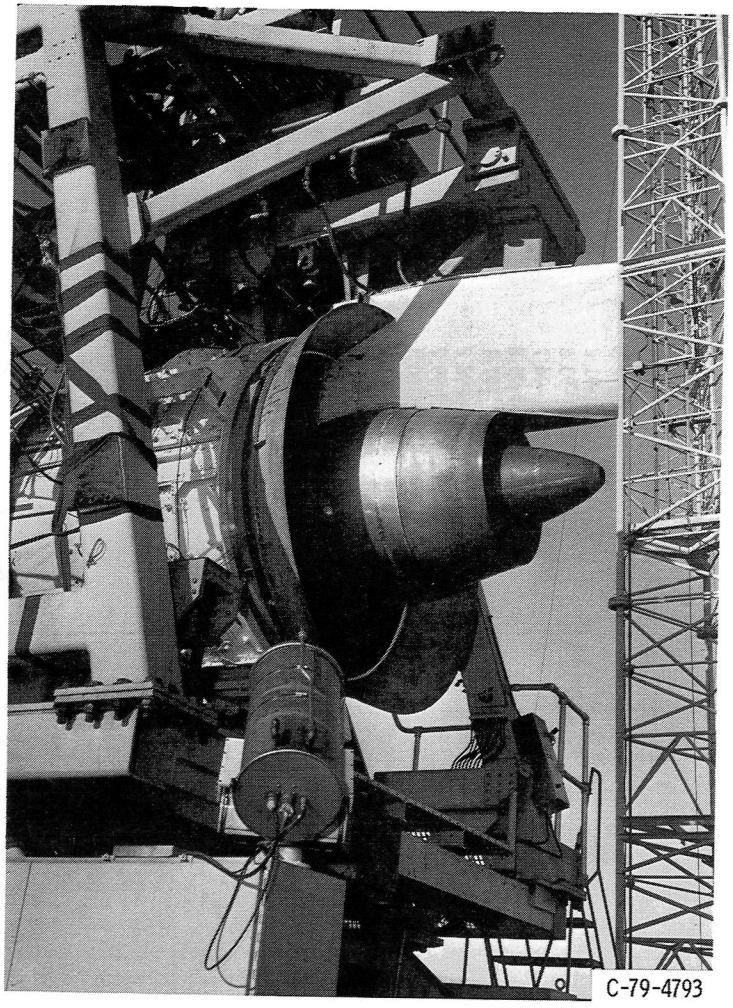

Figure 12. - Fixed 30° exlet on-test.

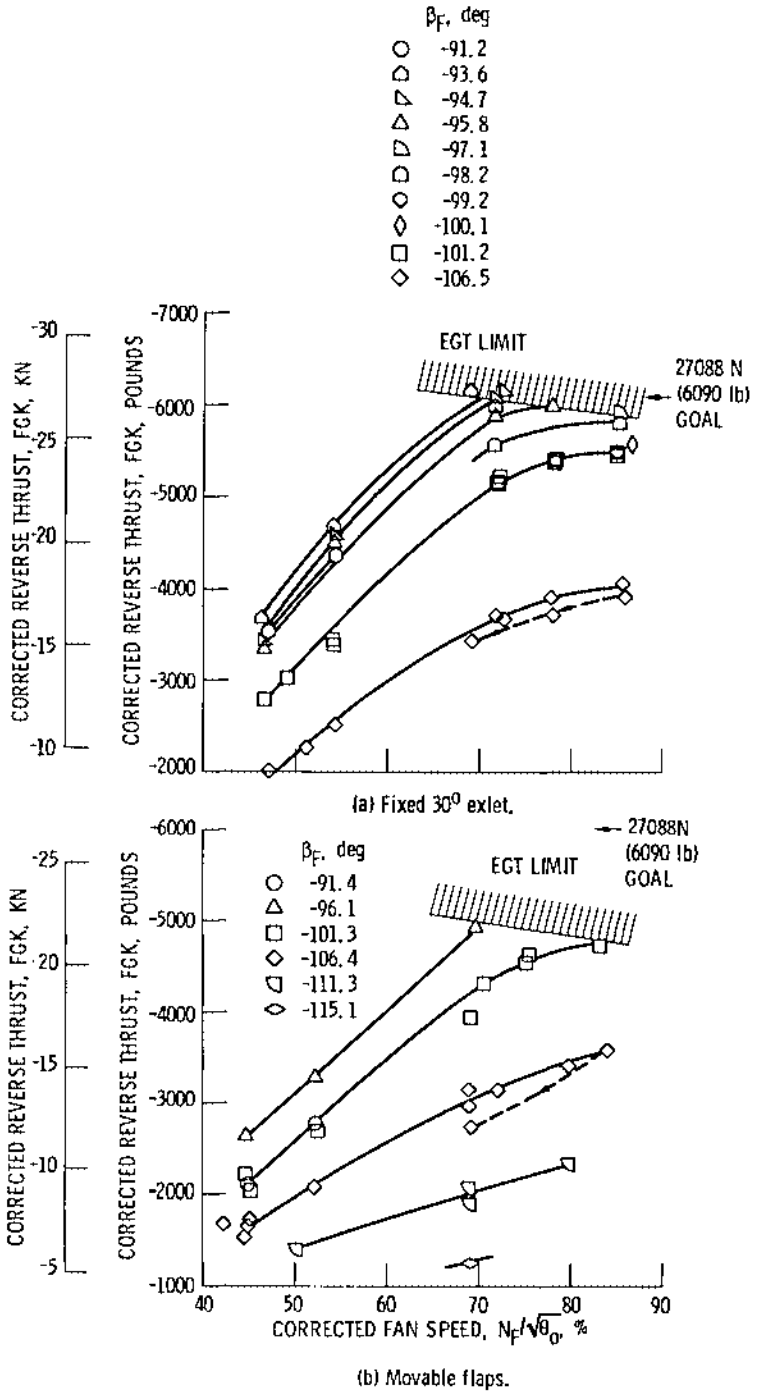

(a) Fixed 30° exlet.

(b) Movable flaps.

Figure 13. - Reverse thrust-fan speed characteristics.

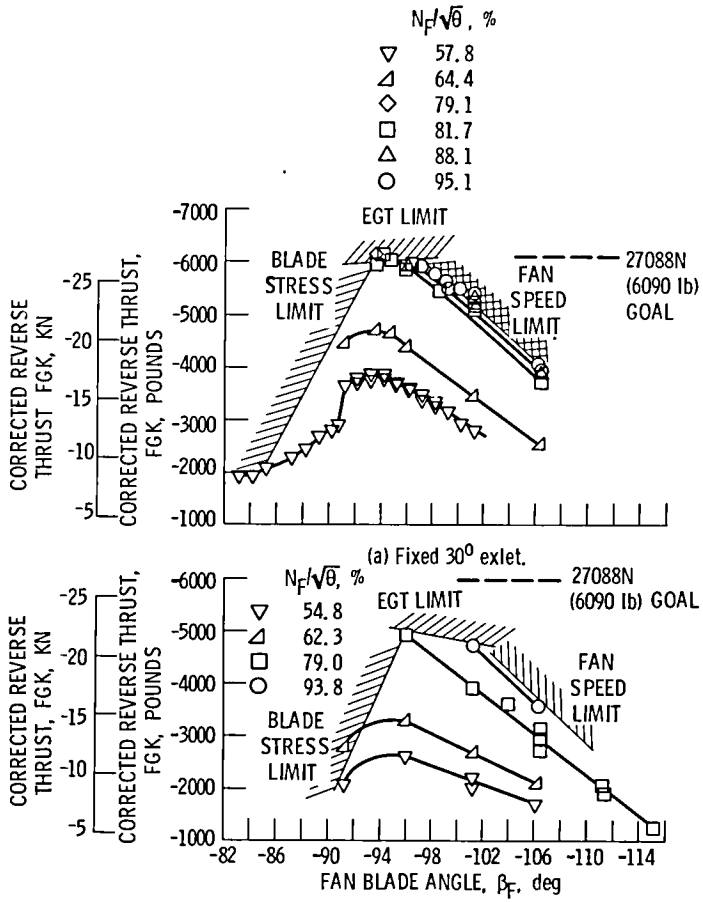

(b) Movable flaps.

Figure 14. - Reverse thrust-fan blade angle characteristics.

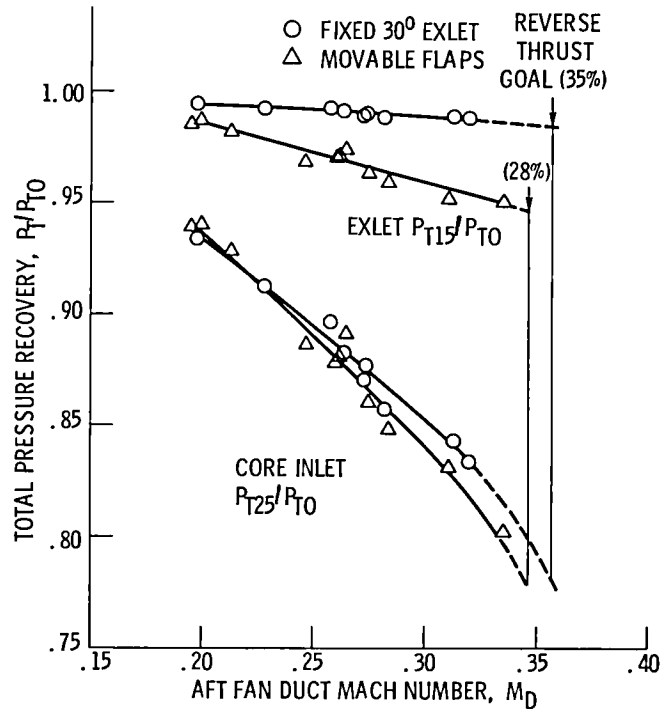

Figure 15. - Exlet and core inlet average total pressure recovery.

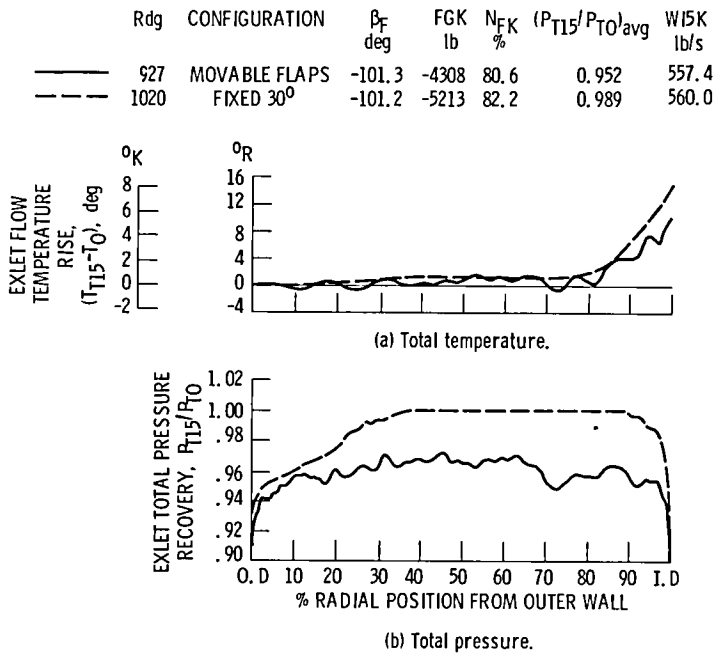

(a) Total temperature.

(b) Total pressure.

Figure 16. - Pressure recovery profiles at fan inlet (STA 15).

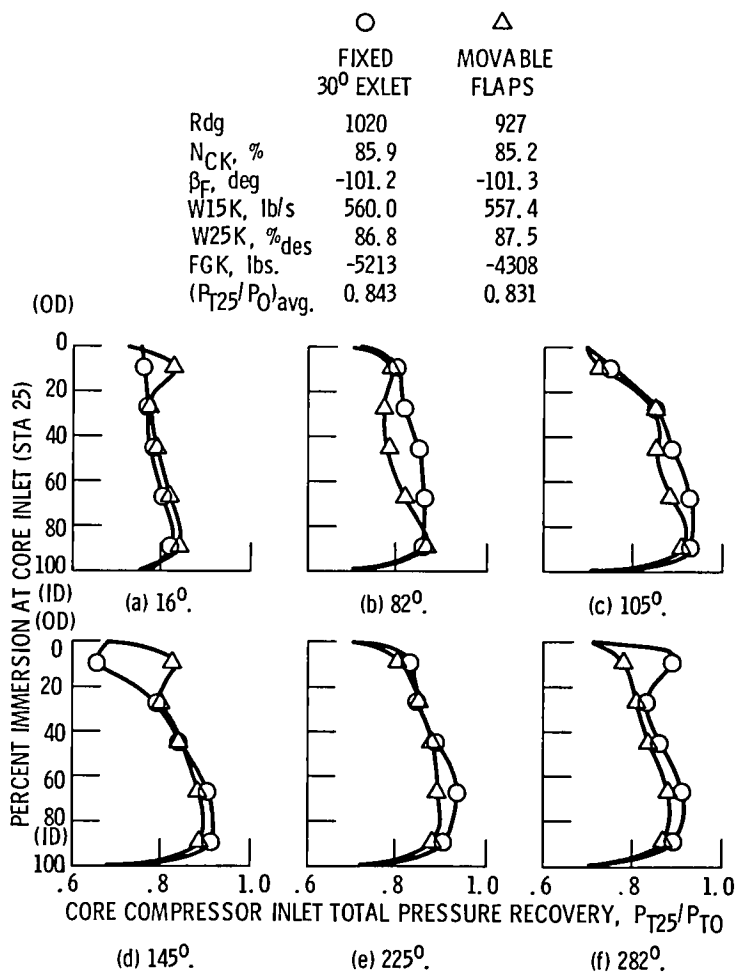

(a) 16°. (b) 82°. (c) 105°.

(d) 145°. (e) 225°. (f) 282°.

Figure 17. - Pressure recovery profiles at core inlet.

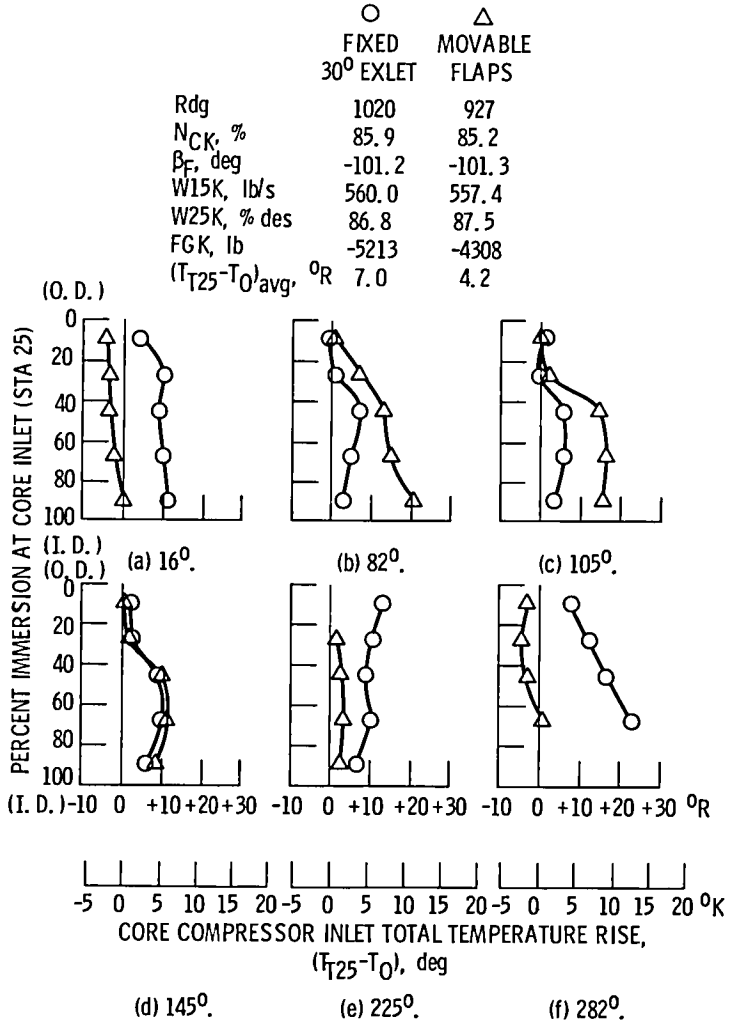

Figure 18. - Compressor inlet total temperature profiles.

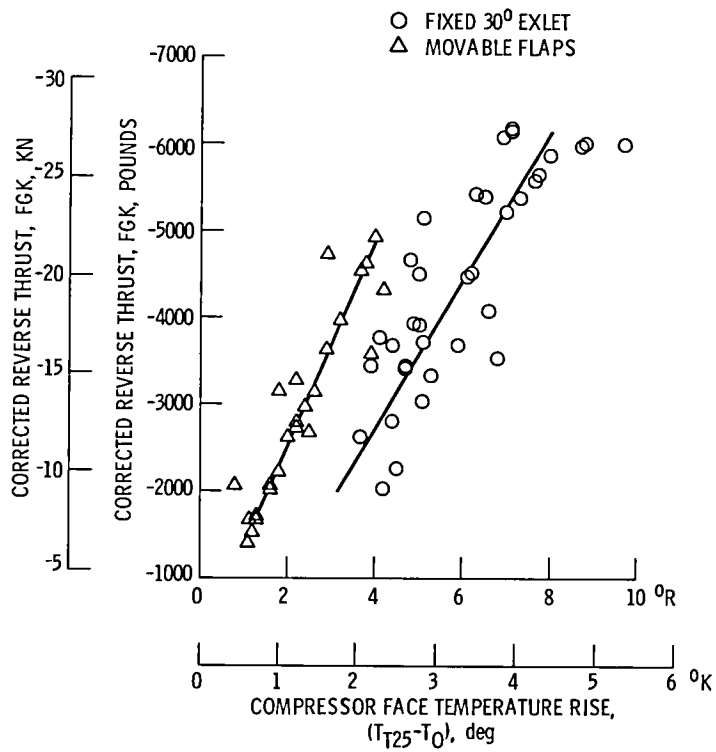

Figure 19. - Average total temperature rise at compressor inlet.

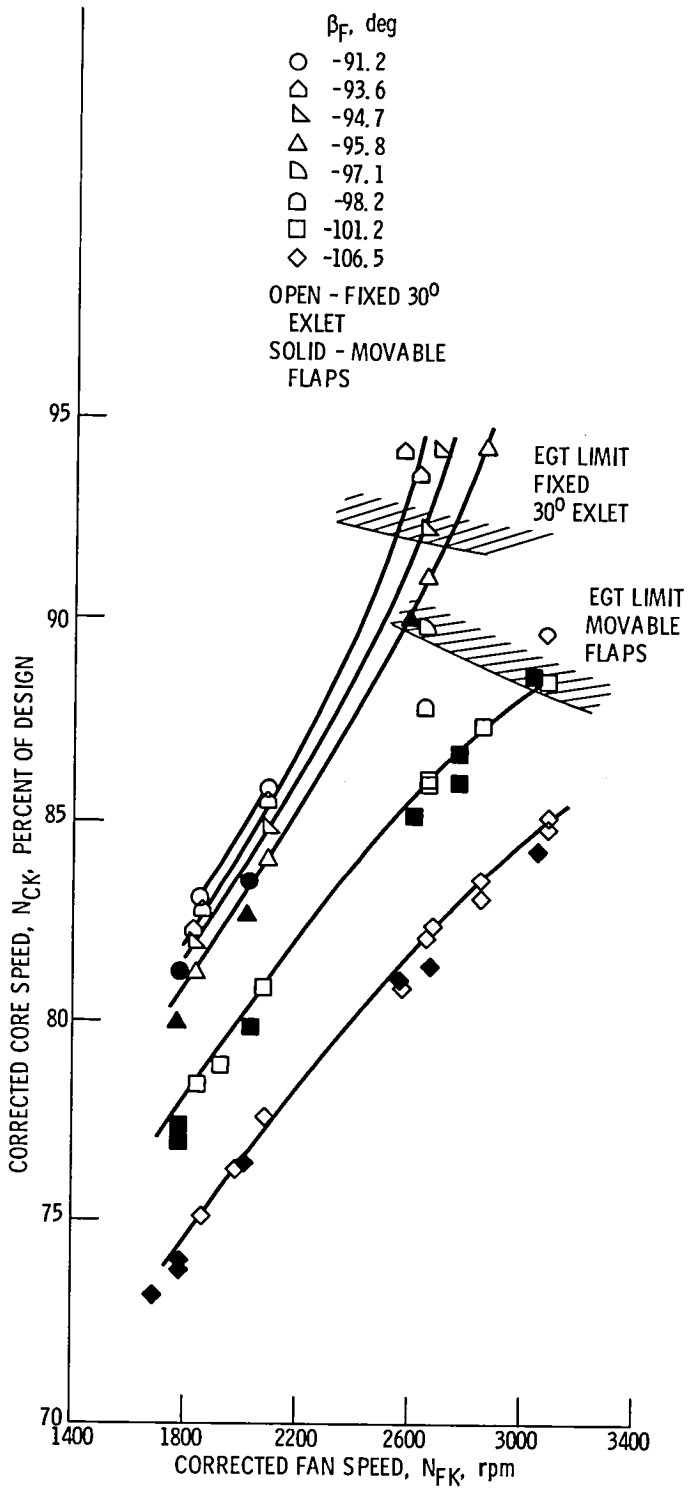

Figure 20. - Fan speed-core speed characteristics.

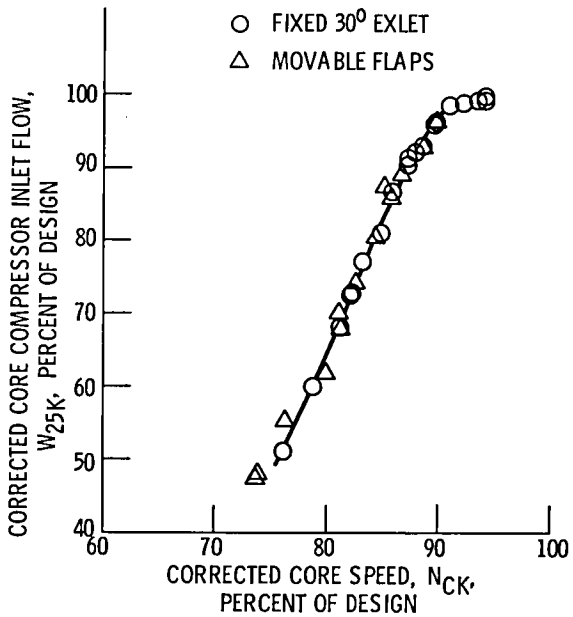

Figure 21. - Compressor flow-speed characteristics.

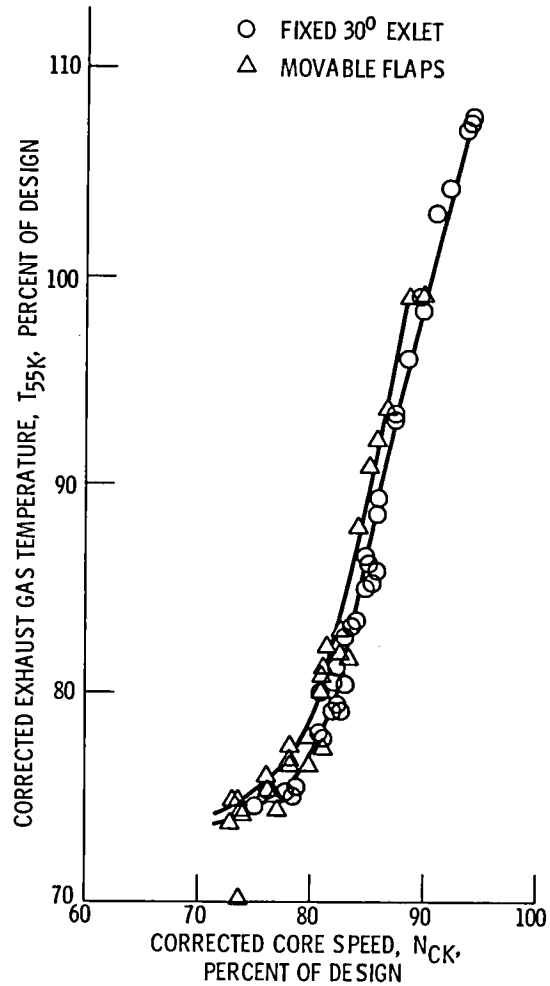

Figure 22. - Exhaust gas-core speed characteristics.

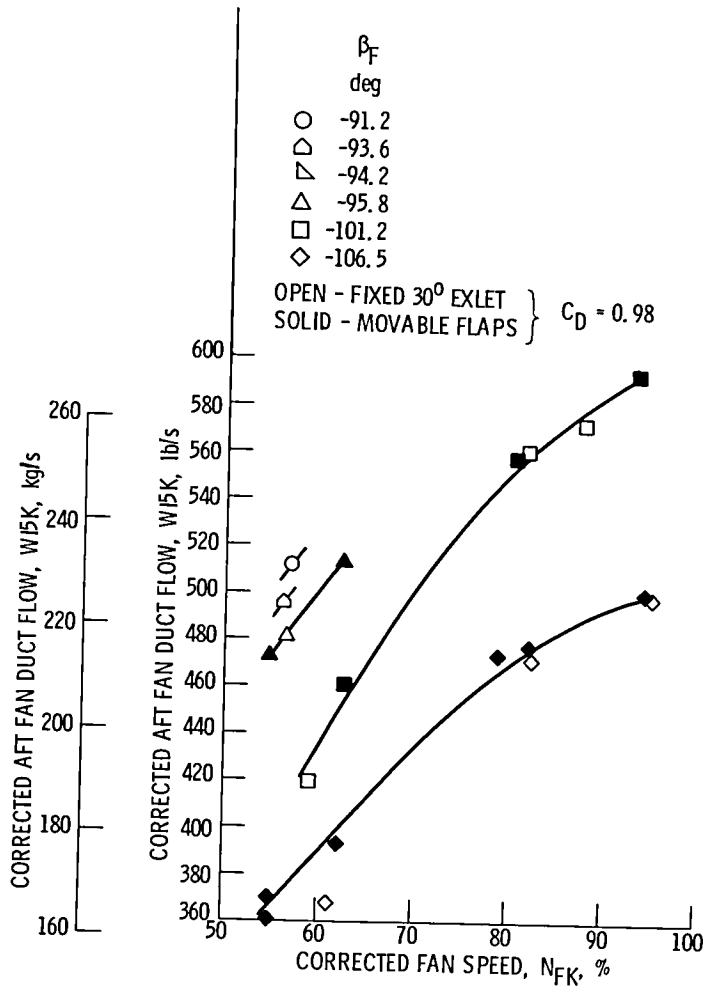

Figure 23. - Reverse air flow-fan speed characteristics.

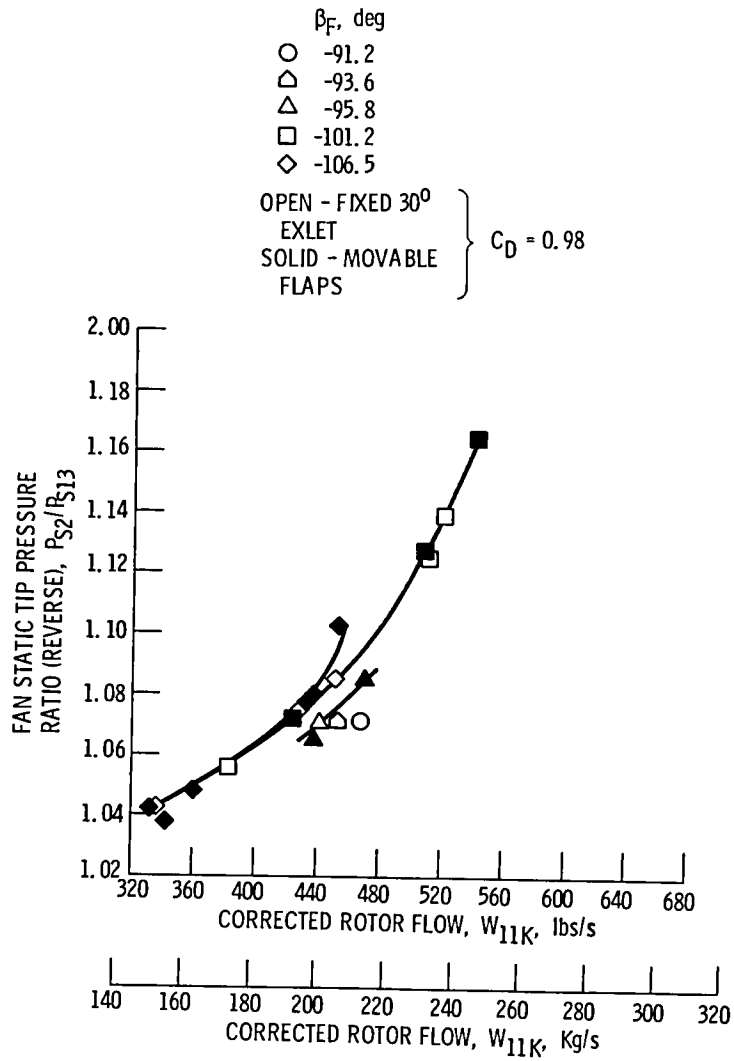

Figure 24. - Fan static pressure ratio-flow characteristics.

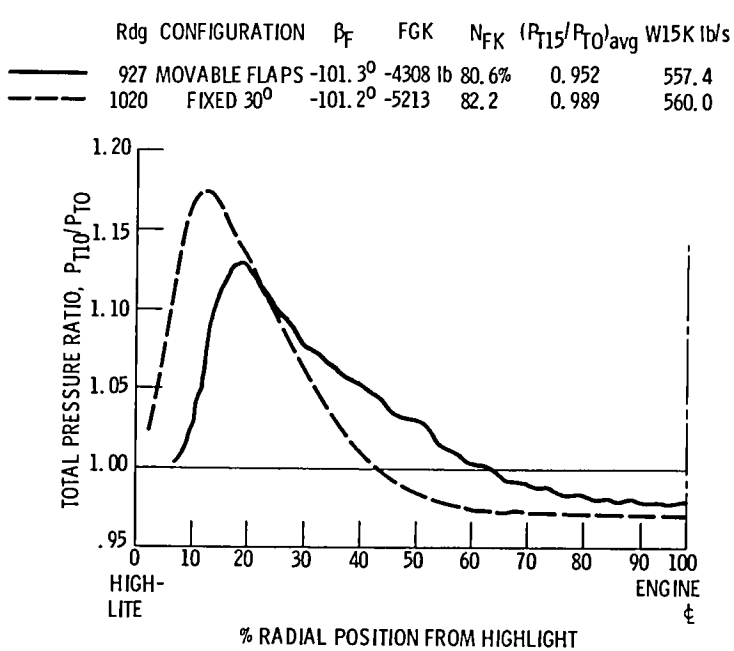

Figure 25. - Total pressure profiles at fan nozzle discharge (inlet highlight).

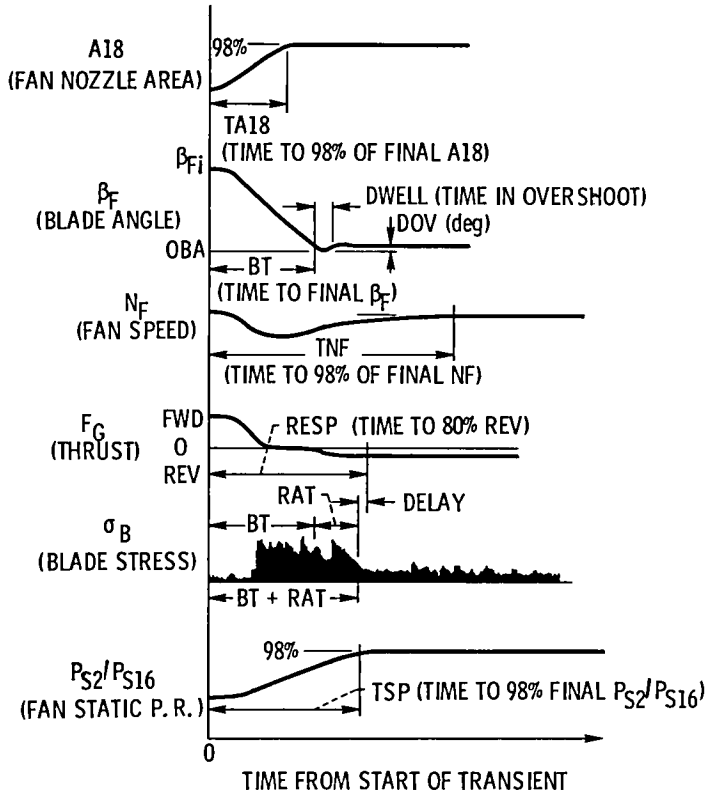

Figure 26. - Nomenclature for forward-to-reverse thrust transients.

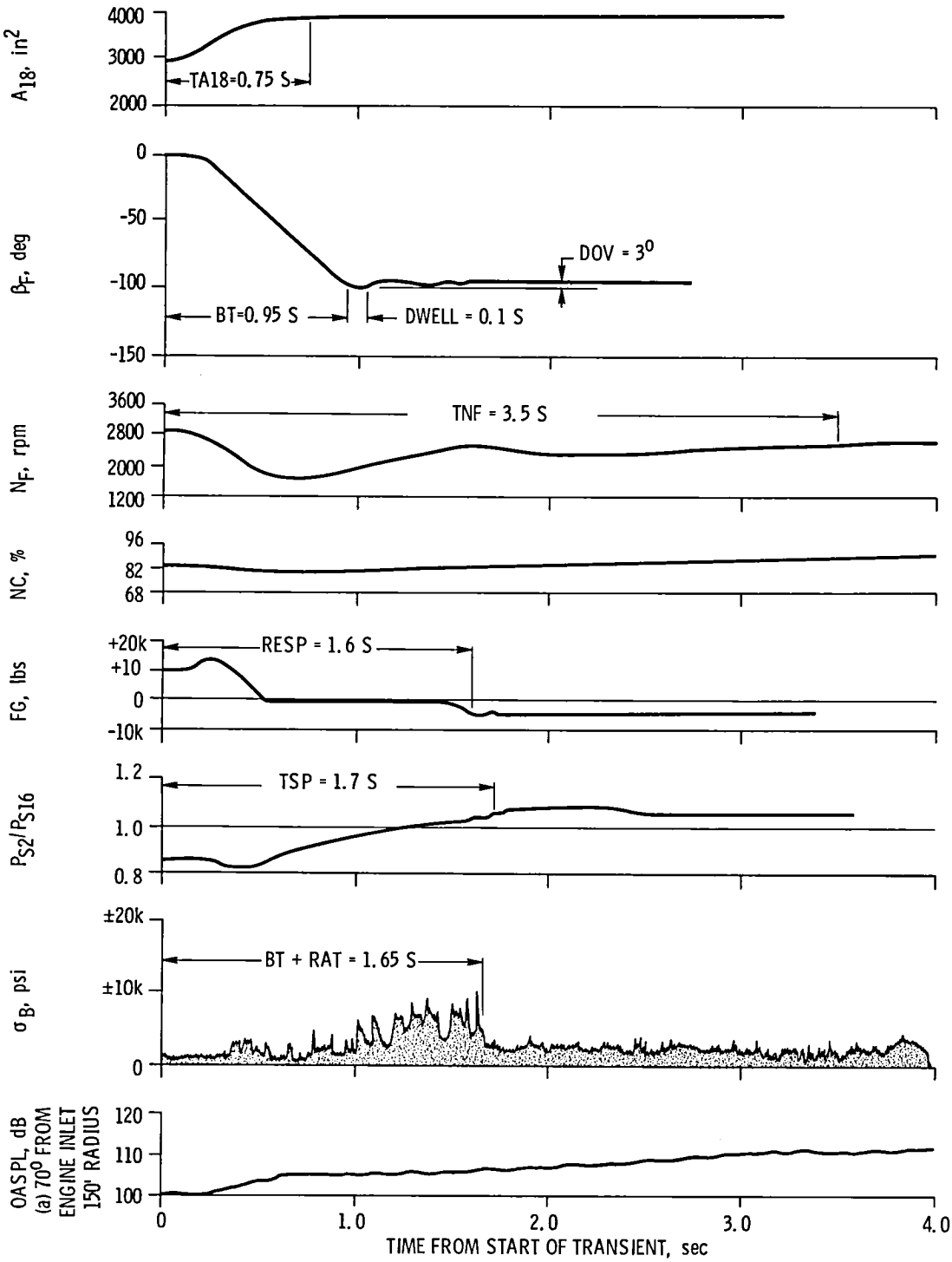

Figure 27. - Approach-to-reverse transient (#15) with no blade overshoot.

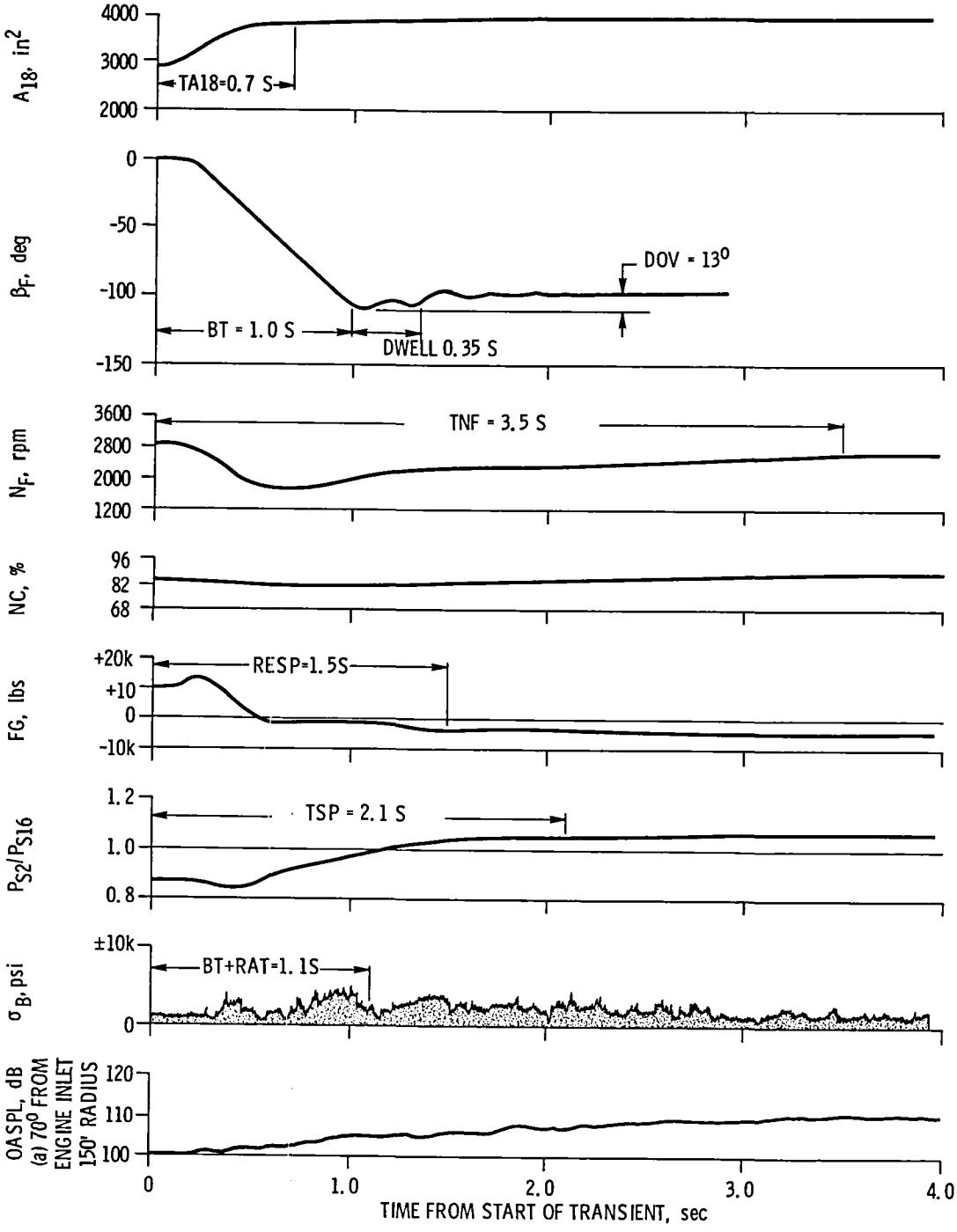

Figure 28. - Approach-to- reverse transient (#14) with 10° blade overshoot.

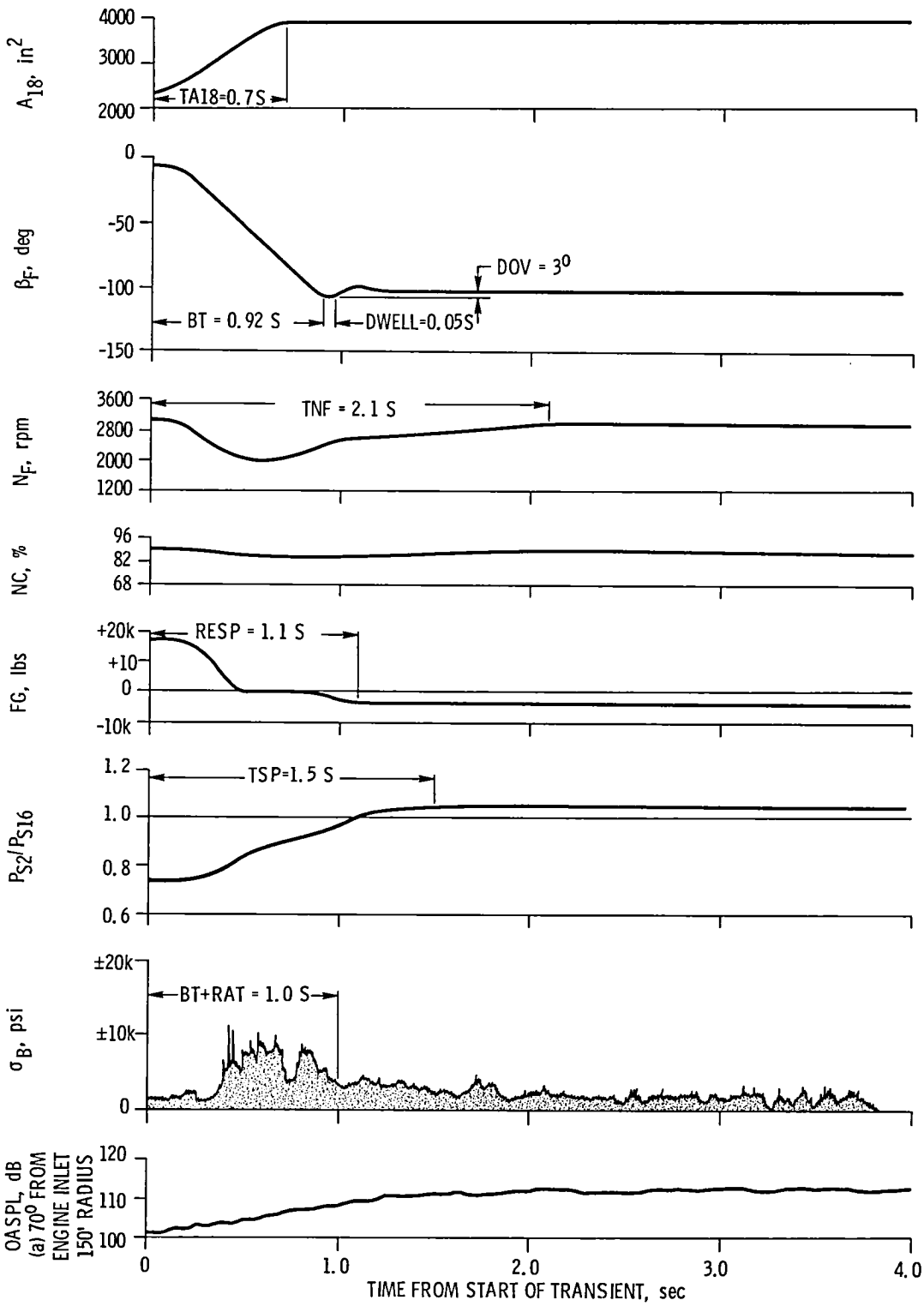

Figure 29. - Takeoff-to-reverse transient (#13) with no blade overshoot.

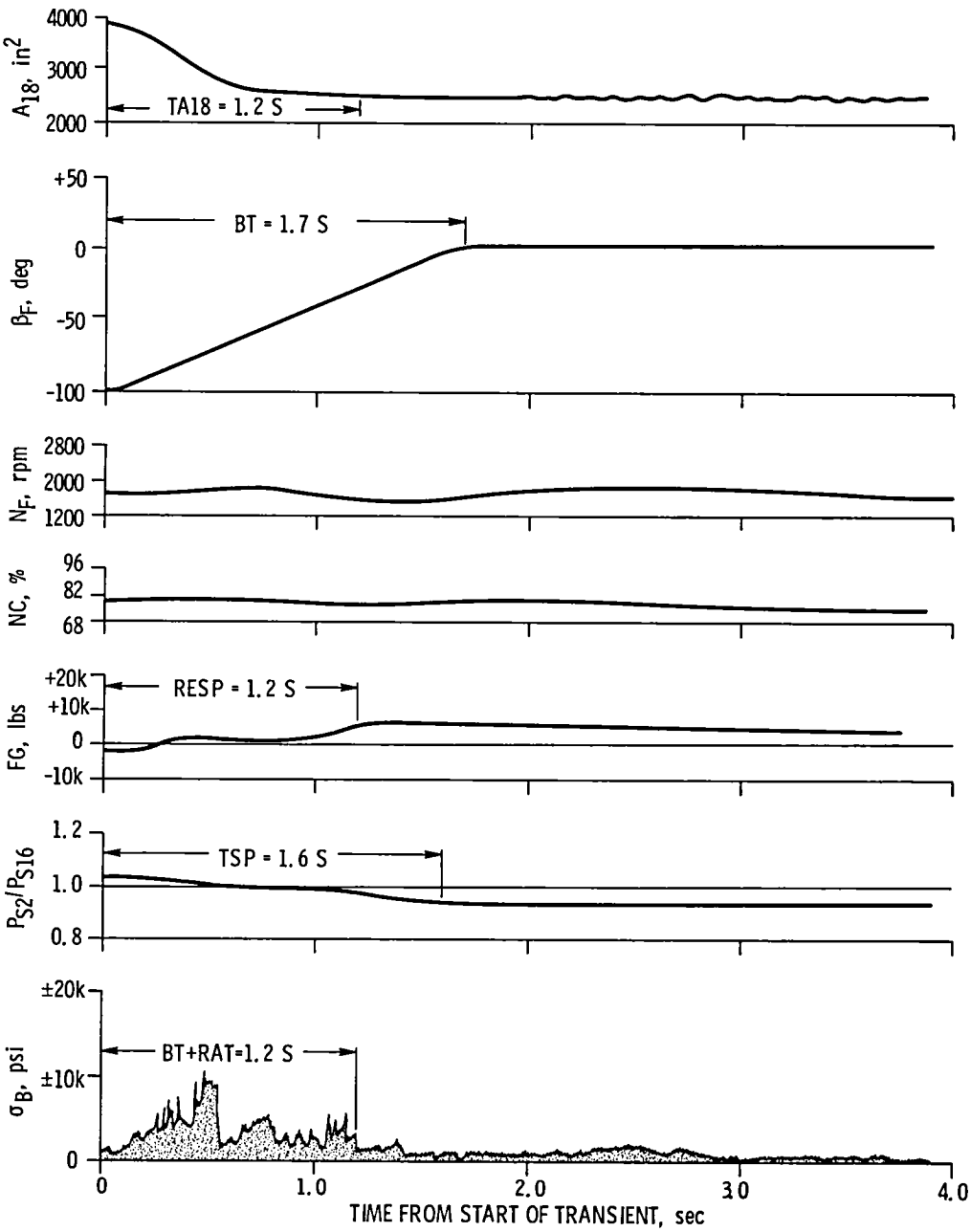

Figure 30. - Typical reverse idle-to-forward idle transient.

TRANS #	BLADE OVER-SHOOT	FUEL INTER-LOCK	INITIAL (FWD) β_F deg	N_{FK} %	FGK lb	FINAL (REV) β_F deg	N_{FK} %	FGK lb
5	NO	-90	+5.3	56.5	4546	-101.6	90.5	-4626
13	NO	-70	-7.2	95.5	17 136	-101.5	89.5	-4607
15	NO	-70	+3.1	88.5	10 632	-96.8	81.2	-4945

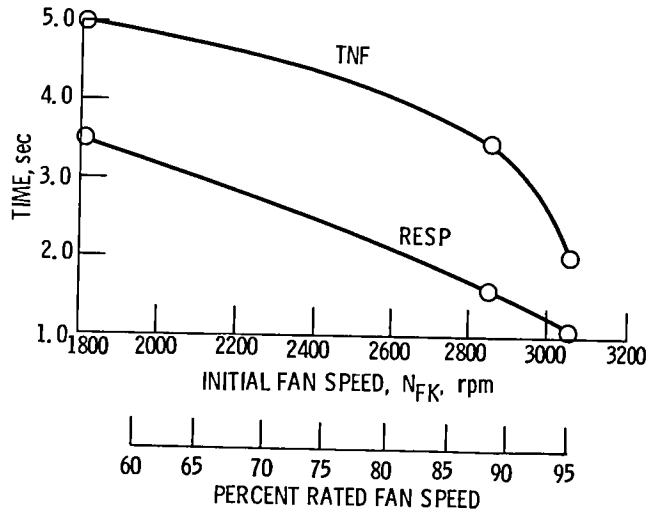

Figure 31. - Effect of initial fan speed on response characteristics during forward-to-reverse transient.

TRANS #	BLADE OVER-SHOOT	FUEL INTER-LOCK	INITIAL (FWD) β_F, deg	N_{FK} %	FGK lb	FINAL (REV) β_F deg	N_{FK} %	FGK lb
1	NO	-90	+5.2	57.0	4579	-101.6	56.6	-2173
2	NO	-90	+5.0	57.0	4644	-101.4	56.7	-2359
3	NO	-90	+5.1	56.9	4650	-101.4	65.4	-3074
4	NO	-90	+5.1	56.8	4517	-101.7	82.2	-4444
5	NO	-90	+5.3	56.5	4546	-101.6	90.5	-4626

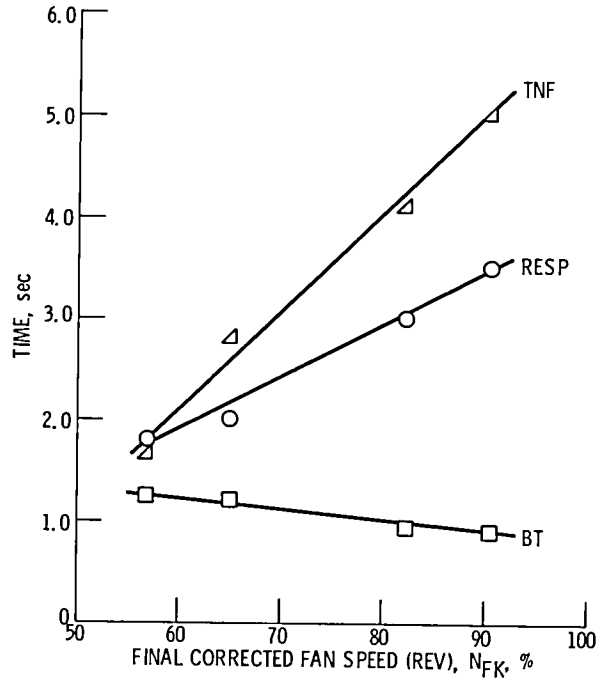

Figure 32. - Effect of final final fan speed on response characteristics.

TRANS #	BLADE OVER-SHOOT	FUEL INTER-LOCK	INITIAL (FWD) β_F deg	N_{FK} %	FGK lb	FINAL (REV) β_F deg	N_{FK} %	FGK lb
7	NO	-70	+2.3	88.2	10 662	-101.4	89.8	-4506
10	NO	-70	+2.4	88.1	10 750	-111.7	89.7	-2350
12	NO	-70	+2.5	88.2	10 768	-106.7	89.8	-3400
13A	YES	-70	+3.0	88.0	10 765	-87.0	80.9	0

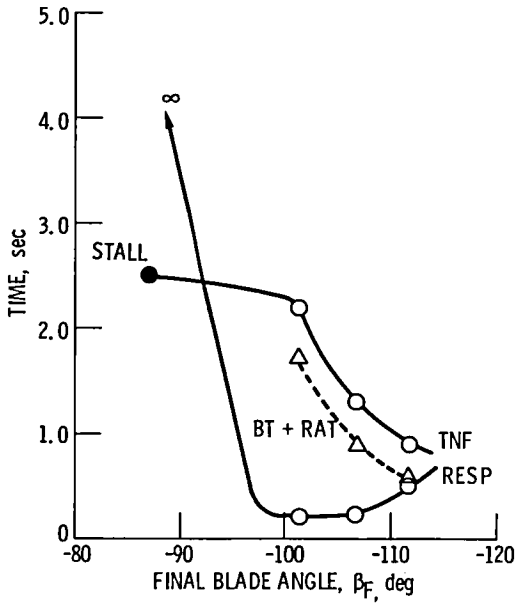

Figure 33. - Effect of final blade angle on response characteristics during approach-to-reverse transients.

	TRANS #	BLADE OVER-SHOOT	FUEL INTER-LOCK	INITIAL (FWD) β_F deg	N_{FK} %	FGK lb	FINAL (REV) β_F deg	N_{FK} %	FGK lb
○	7	NO	-70	+2.3	88.2	10 662	-101.4	89.8	-4506
○	9	YES	-70	+2.5	88.1	10 660	-101.9	89.7	-4256
△	14	YES	-70	+3.1	88.9	10 630	-96.8	81.2	-4940
△	15	NO	-70	+3.1	88.5	10 632	-96.8	81.2	-4945
□	16	NO	-50	+3.1	88.9	10 083	-101.8	90.4	-4331
□	17	YES	-50	+3.4	88.7	10 375	-101.8	90.3	-4292

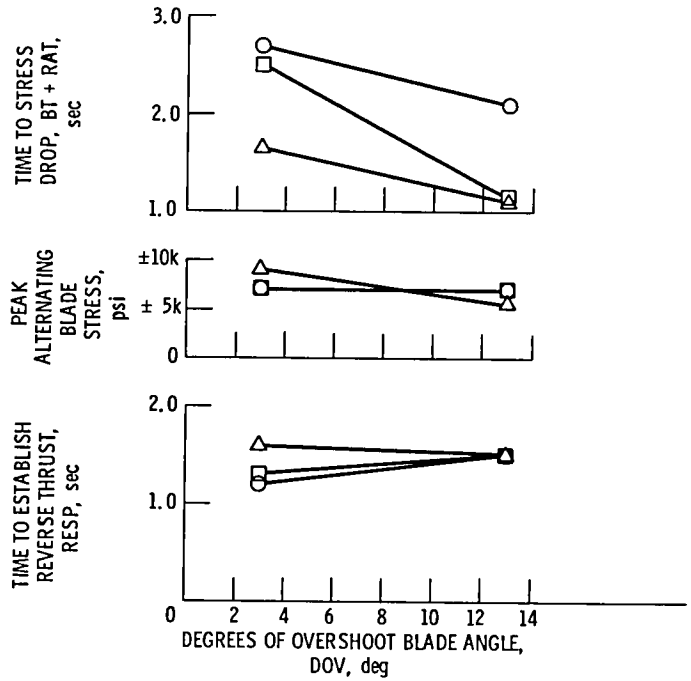

Figure 34. - Effect of fan blade overshoot on thrust response and blade stress characteristics during forward-to-reverse transient.

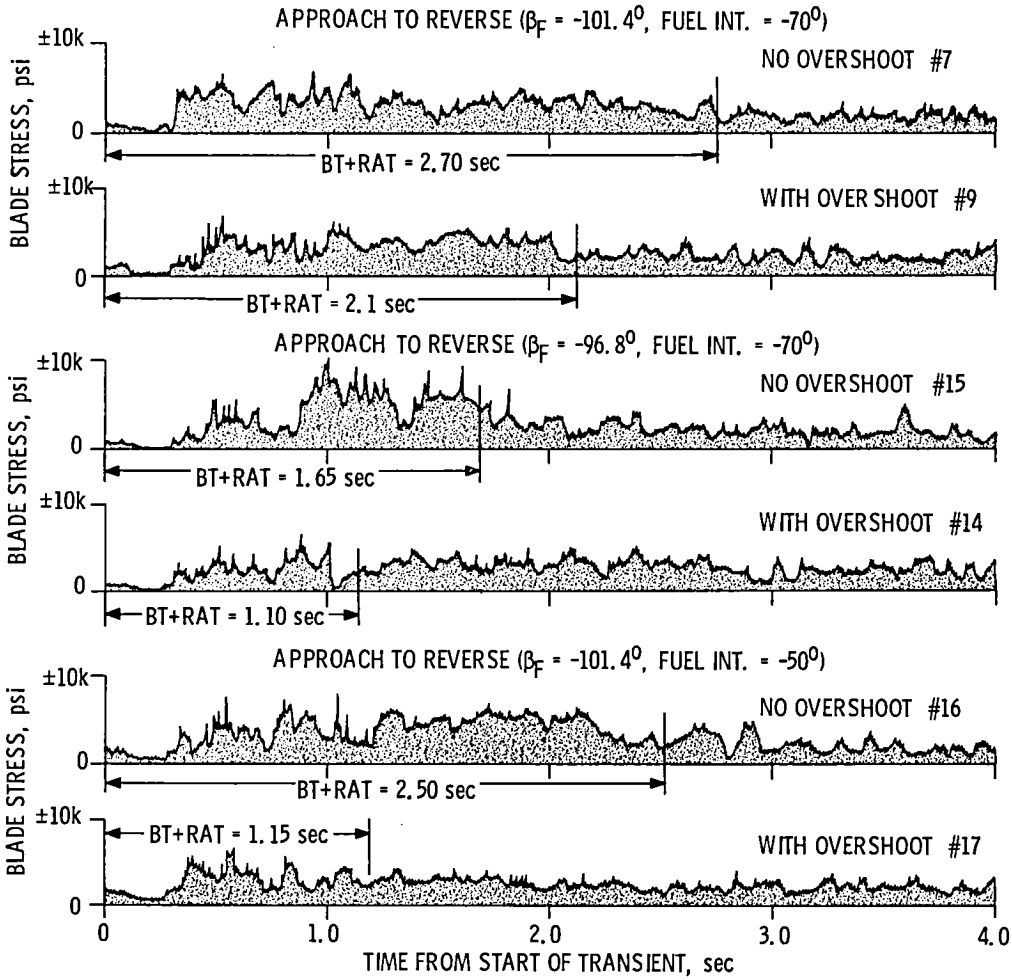

Figure 35. - Fan blade stress during forward-to-reverse transient with and without blade overshoot.

TRANS #	BLADE OVER-SHOOT	FUEL INTER-LOCK	INITIAL (FWD) β_F deg	N_{FK} %	FGK lb	FINAL (REV) β_F deg	N_{FK} %	FGK lb
6	NO	-90	+2.6	88.5	10 077	-101.4	89.9	-4474
7	NO	-70	+2.3	88.2	10 662	-101.4	89.8	-4506
8	NO	-60	+2.5	88.3	10 683	-101.7	89.7	-4695
16	NO	-50	+3.1	88.9	10 083	-101.8	90.4	-4331

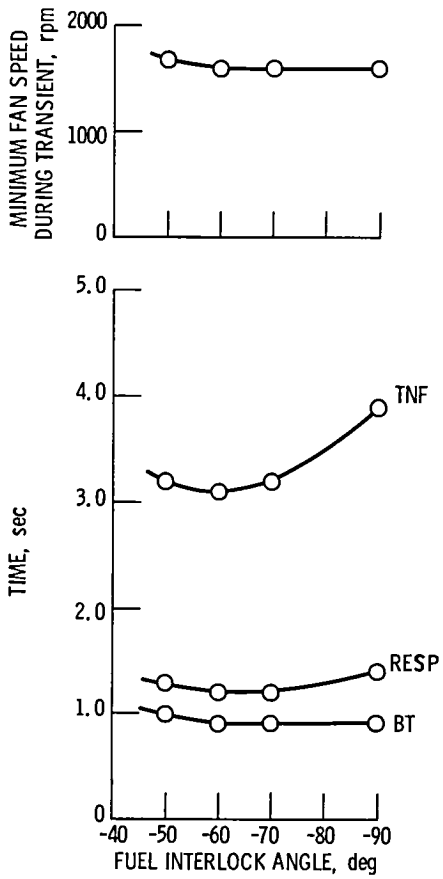

Figure 36. - Effect of fuel scheduling during forward-to-reverse transient on fan speed excursions and response characteristics.

1. Report No.	2. Government Accession No.	3. Recipient's Catalog No.
NASA TM-81558		

4. Title and Subtitle	5. Report Date
REVERSE THRUST PERFORMANCE OF THE QCSEE VARIABLE PITCH TURBOFAN ENGINE	6. Performing Organization Code

7. Author(s)	8. Performing Organization Report No.
N. E. Samanich, D. C. Reemsnyder, and H. E. Bloomer	E-519

9. Performing Organization Name and Address	10. Work Unit No.
National Aeronautics and Space Administration Lewis Research Center Cleveland, Ohio 44135	11. Contract or Grant No.

12. Sponsoring Agency Name and Address	13. Type of Report and Period Covered
National Aeronautics and Space Administration Washington, D.C. 20546	Technical Memorandum
	14. Sponsoring Agency Code

15. Supplementary Notes

Prepared for the Aerospace Congress sponsored by the Society of Automotive Engineers, Los Angeles, California, October 13-16, 1980.

16. Abstract

Results of steady-state reverse and forward-to-reverse thrust transient performance tests are presented. The original QCSEE 4-segment variable fan nozzle was retested in reverse and compared with a continuous, 30^{o} half-angle conical exlet. Data indicated that the significantly more stable, higher pressure recovery flow with the fixed 30^{o} exlet resulted in lower engine vibrations, lower fan blade stress and approximately a 20 percent improvement in reverse thrust. Objective reverse thrust of 35 percent of takeoff thrust was reached. Thrust response of less than 1.5 sec was achieved for the approach and the takeoff-to-reverse thrust transients.

17. Key Words (Suggested by Author(s))	18. Distribution Statement
Aircraft propulsion Powered lift systems Engine reverse thrust tests Thrust transients	Unclassified - unlimited STAR Category 07

19. Security Classif. (of this report)	20. Security Classif. (of this page)	21. No. of Pages	22. Price*
Unclassified	Unclassified		

* For sale by the National Technical Information Service, Springfield, Virginia 22161